Horizon 2020 - LCE-2016-2017 - Competitive Low-Carbon Energy

FLEXCoop

Democratizing energy markets through the introduction of innovative flexibility-based demand response tools and novel business and market models for energy cooperatives

WP3 – Demand Flexibility Modelling and Forecasting

D3.1 Models of DER Devices and associated Forecasting Algorithms

Due date: 31.07.2018 **Delivery Date**: 17.08.2018

Author(s): Rishi Relan (DTU), Armin Ghasem Azar (DTU), Peder Bacher (DTU), Henrik Madsen (DTU), Katerina Valalaki (Hypertech), Tasos Tsitsanis (Hypertech), Kostas Tsatsakis (Hypertech), Tsiakoumi Matina (Hypertech), Gregorio Fernández Aznar (CIRCE)

Editor: Peder Bacher (DTU)

Lead Beneficiary of Deliverable: DTU

Dissemination level: Public **Nature of the Deliverable:** Report

Internal Reviewers: Armin Wolf (Fraunhofer), Dimitris Panopoulos (S5),

FLEXCOOP Key Facts

Topic:	H2020-LCE-2016-2017 - Competitive Low-Carbon Energy
Type of Action:	Research and Innovation Action
Project start:	01 October 2017
Duration:	36 months from **01.10.2017** to **30.09.2020** (Article 3 GA)
Project Coordinator:	Fraunhofer
Consortium:	13 organizations from nine EU member states

FLEXCOOP CONSORTIUM PARTNERS

Fraunhofer	Fraunhofer-Gesellschaft zur Förderung der angewandten Forschung e.V.
ETRa	ETRA INVESTIGACION Y DESARROLLO SA
HYPERTECH	HYPERTECH (CHAIPERTEK) ANONYMOS VIOMICHANIKI
DTU	DANMARKS TEKNISKE UNIVERSITET
GRINDROP	GRINDROP LIMITED
CIRCE	FUNDACION CIRCE CENTRO DE INVESTIGACION DE RECURSOS Y CONSUMOS ENERGETICOS
KONCAR	KONCAR - INZENJERING ZA ENERGETIKUI TRANSPORT DD
SUITE5	SUITE5 DATA INTELLIGENCE SOLUTIONS Limited
S5	SUITE5 DATA INTELLIGENCE SOLUTIONS Ltd
CIMNE	CENTRE INTERNACIONAL DE METODES NUMERICS EN ENGINYERIA
RESCOOP.EU	RESCOOP EU ASBL
SomEnergia	SOM ENERGIA SCCL
ODE	ORGANISATIE VOOR HERNIEUWBARE ENERGIE DECENTRAAL
Escozon	ESCOZON COOPERATIE UA - affiliated or linked to ODE
MERIT	MERIT CONSULTING HOUSE SPRL

Disclaimer: FLEXCOOP is a project co-funded by the European Commission under the Horizon 2020-LCE-2017-SGS - Competitive Low-Carbon Energy Programme under Grant Agreement No. 773909.

The information and views set out in this publication are those of the author(s) and do not necessarily reflect the official opinion of the European Communities. Neither the European Union institutions and bodies nor any person acting on their behalf may be held responsible for the use, which may be made of the information contained therein.

© Copyright in this document remains vested with the FLEXCOOP Partners

EXECUTIVE SUMMARY

The goal of this document is to present and analyse Distributed Energy Resources (DER) device models along with the relevant processes required to define and formalise their control and response capabilities towards defining their flexibility capacity in demand response programmes. The DER models are divided into: demand, storage and generation.

Demand models refer to residential loads with significant capacity to affect the building-level energy demand and provide flexibility as well as support the indoor environment optimisation in terms of comfort and health preservation. To this end, Heating, Ventilation and Air Condition (HVAC) and lighting have been identified as the most suitable loads. The FLEXCoop DER load models contain the mathematical formulas for the calculation of electric demand (consumption) of each DER type as a function of dynamic (input data) and static (configuration) parameters affecting DER operation. A training period, gathering data from the physical devices is required towards the extraction of the configuration parameters. The FLEXCoop load modelling framework will allow for continuous calibration of the respective DER models in order to account for efficient and effective dynamic adaptation to potential shifts in the "behaviour" of the corresponding physical entities (seasonal patterns, device performance degradation, etc).

Storage models refer to stationary Energy Storage Systems (ESS) and Vehicle-as-ESS. Vehicle-as-ESS basically means, that electrical vehicle batteries are used in a very similar manner, as stationary batteries. Therefore, it provides the same services such as: integration of renewable generation, grid services such as voltage and frequency control, supply emergency backup power, peak shaving and valley filling, to give some examples. First, the stationary system is described (incorporating both economic and thermodynamic parameters) and aligned with FLEXCoop business scenarios. Then, additional model variables are introduced, in order to consider peculiarities of the electric vehicles.

The generation forecasting models presented in the document aim to describe the behaviour of small generators available in the FLEXCoop pilot dwellings and in the portfolio of energy cooperatives. For the pilot dwellings that we have currently identified only residential Photo Voltaics (PVs) are available. Thus, we have chosen to analyse only PV generation forecasting in the deliverable. However, if during the project implementation, wind generation units identified and need to be incorporated in the overall FLEXCoop solution demonstration, the proposed algorithms will appropriately be adapted to fulfil this additional requirement. The models can be applied to provide short and very short-term forecasting of PV generation in an automatic and effective way, both in terms of performance and computational resources.

Table of Contents

LIST OF FIGURES

LIST OF TABLES

CODE LISTINGS

ABBREVIATIONS

BES	Battery Energy System
BMS	Battery Management System
CO	Confidential, only for members of the Consortium (including the Commission Services)
COP	Coefficient of Performance
DER	Distributed Energy Resources
DHW	Domestic Hot Water
DoW	Description of Work
EV	Electric Vehicle
ESS	Energy Storage System
HVAC	Heating, Ventilation and Air Condition
LV	Low Voltage
NWP	Numerical Weather Prediction
O&M	Operation and Maintenance
PV	Photo Voltaic
SoC	Stage of Charge
V2G	Vehicle-to-Grid
WP	Work Package

1. INTRODUCTION

For energy systems to become "smart" and "intelligent", meaning that they are able to react on signals from the surrounding systems, one of the most critical aspects is to have efficient and accurate models for modelling and forecasting. Both models for load (e.g. light and heating), storage (e.g. batteries) and generation (e.g. Photo Voltaic (PV) and wind generation) are important, naturally, depending on which components are in the particular system. In the FLEXCoop project the focus is on single-family dwellings and in the report models and modelling techniques, which will be applied in the operation of the pilot sites, are presented. Naturally, the models presented here are not yet fitted and tuned for the particular FLEXCoop pilot sites, however the basic concepts and approaches are described in detail and their applicability are shown in examples using relevant data from other sources.

A short introduction and literature review for each of the application contexts: load, storage and generation, are included in the respective sections.

The report starts by setting the scene, first by presenting the objectives in Section 2 and in Section 3 an overview of how the different models and data flows in the FLEXCoop setup will interact is given. In Section 4 the load models are presented, in detail both of lighting and heating, and in Section 5 the storage models to be applied are described, they cover both the use of stationary and Electrical Vehicle (EV) batteries. In Section 6 the techniques for generation forecasting are presented. The emphasis is on a detailed description of how to include Numerical Weather Predictions (NWPs) as inputs to statistical forecast models and how the models can be setup in a generic way. As previous explained the focus is on solar forecasting, however the same algorithms can be applied for other types of generation. Finally, in Section 7 the conclusions are drawn.

2. CONCEPT AND DELIVERABLE OBJECTIVES

The deliverable D3.1 on hand "Models of DER Devices and associated Forecasting Algorithms", presents the Distributed Energy Resource (DER) load, generation and storage models came as a result of the respective task T3.1 "DER Modelling and Forecasting Algorithms". As defined in the Description of Work (DoW), this task thoroughly analyses and develops the DER models and the relevant forecasting algorithms that are needed towards finally enabling decision-making optimisation (for the flexibility that needs to be activated) on the aggregator side. The DER models examined include:

- Load models and more specifically lighting and Heating, Ventilation and Air Condition (HVAC) load models
- Storage models including batteries and Electrical Vehicles (EVs)
- Generation forecasting found till now in the pilot dwellings namely residential PV systems

The work-package objective that has been covered is: To further improve and enrich existing DER models allowing the representation and quantification of control and response capabilities and flexibility capacity of a wide range of DERs involved in the FLEXCoop project, while facilitating DER forecasting and aggregation operations on the basis of more robust and accurate models.

3. DEPENDENCIES ON OTHER TASKS – MODELS AND DATA FLOWS

The aim of this section is twofold:

- To present the dependencies of this task on other tasks of the Work Package 3 (WP3). This will guide us throughout the project development to know exactly what is going to be developed in each task and how this is related with the other tasks and the overall scope of the project;
- To describe briefly the different models that are going to be developed in the WP3 and conceptually illustrate the sequence that are going to be used towards finally extracting the context-aware demand flexibility profiles of the residential prosumers examined in the project . As the project progresses, this will be used to link the different models towards providing the FLEXCoop holistic context-aware flexibility profiling framework.

During the development of the WP3, we identified the need to clearly define what we should expect from each task and how the work performed in this task impacts the work that needs to be done in the other tasks to ensure that all of them can be well combined without any logical or technical gaps. Indeed, the different tasks of the WP3 are all somehow correlated (as illustrated in Figure **1**) and only a continuous loop feedback process will result on the construction of robust demand flexibility modelling and forecasting algorithms that could be smoothly incorporated in the FLEXCoop holistic context-aware flexibility profiling mechanism.

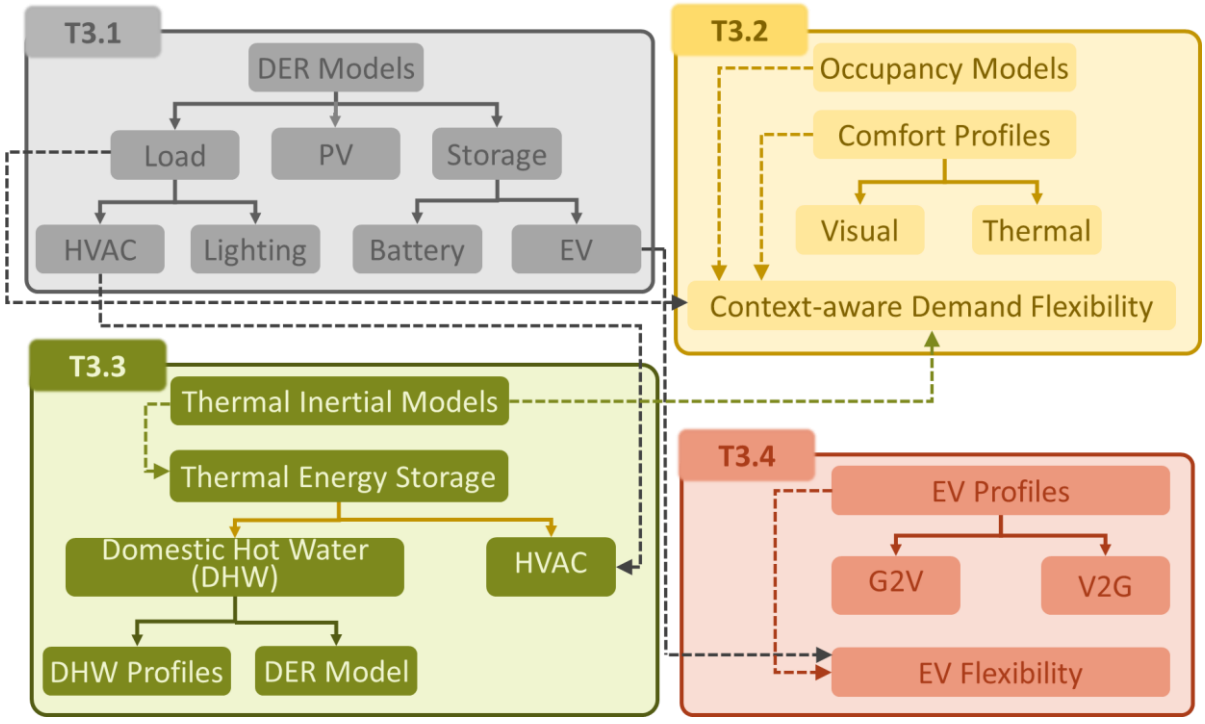

Figure 1: Dependencies of T3.1 on other tasks of the WP3

As already mentioned, T3.1 deals with DER models including load (lighting and HVAC), generation (PV) and storage (batteries, EVs) assets and it is the subject of this deliverable. The overall objective of FLEXCoop, however, is not the models per se but to provide holistic context-aware demand flexibility profiles that will be continuously updated based on real-time energy data. To this end, as it is deduced from Figure **1**, the DER load models developed in

T3.1 and analysed herein, will be combined with the occupancy models and comfort profiles (visual and thermal) that are currently developed in the T3.2. The latter will provide the illuminance and temperature boundaries that will be taken into account to ensure that each individual pilot user will always remain in his/her comfort zone (concerning preferred illuminance and temperature).

To provide context-aware demand flexibility profiles, the DER HVAC models will also need to be combined with the thermal inertia models that are currently constructed in the T3.3. By the term thermal inertia model, we refer to the dynamic thermal modelling of buildings that will define thermal mass/inertia of individual spaces within each specific pilot dwelling. The occupancy and thermal comfort profiles combined with the thermal inertia model of a building space will be used to translate environmental/context conditions and building characteristics to the heat demand required to maintain the indoor temperature in between the user's thermal comfort boundaries (temperature limits identified through thermal comfort profiles). Then, the DER HVAC models will be used to correlate the required heat demand with the electric energy consumption of the HVAC system and thus the flexibility that can be offered. The latter requires also an estimation of a baseline consumption as this will be further analysed in T3.2 (in Figure 2, the term "flexibility models" incorporates also the models needed for baselining).

The case of DER lighting devices is more straightforward and the DER model (this includes a space luminance model as it will be explained in more detailed below) combined with the occupancy models and visual comfort profiles can estimate the required electric power and thus the flexibility that can be offered. This is further elaborated in the DER lighting model in the Section 4.4.1.

The sequence of the DER load models as they will be used in FLEXCoop integrated solution along with the main input/output data and how these will flow among the different FLEXCoop models are schematically shown in Figure 2.

Similarly, in Figure 3, the sequence of the DER EV models presented and analysed in this deliverable along with the main input/output data and how these will flow among the different FLEXCoop EV models are shown. As it is deduced from Figure 1 and Figure 3, the T3.1 needs to be combined with the T3.4 towards extracting personalised EV flexibility that will enable the integration of electro mobility in the FLEXCoop DR optimisation functions.

Finally, considering the DER generation modelling, the models presented herein for improved forecasting and analysis of generation DERs at the local and district level can be directly used by the FLEXCoop optimisation framework allowing the deployment of highly efficient DR strategies in specific business cases, as for example those focusing on maximisation of variable renewable energy sources output absorption (self-consumption).

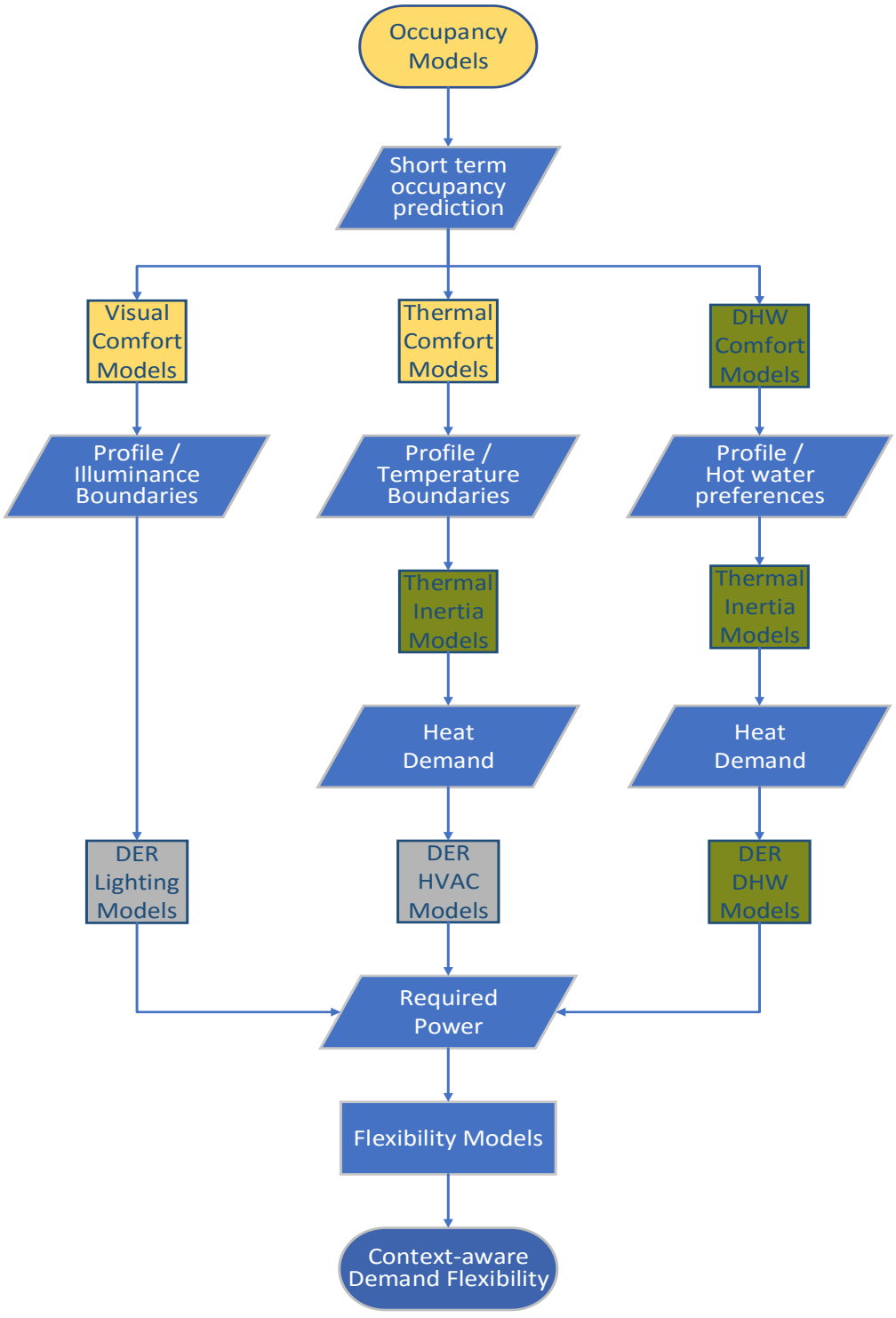

Figure 2: FLEXCoop models sequence towards extracting context-aware demand flexibility[1]

[1] The colors in the flowchart are aligned with the ones of the Figure **1** indicating the Task where each model is developed. Where no alignment exists (blue filled objects), this means that the respective data and/or models are extracted combining the work performed in more than one tasks.

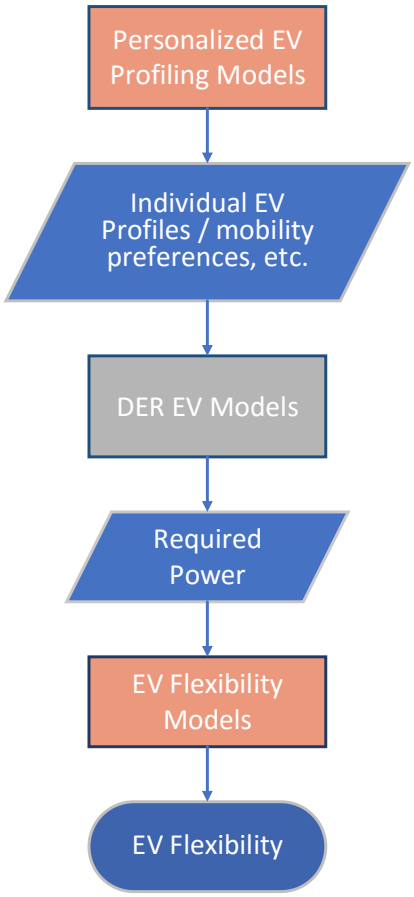

Figure 3: Models sequence and data flow among them towards extracting EV flexibility[2]

[2] The colors in the flowchart are aligned with the ones of the Figure **1** indicating the Task where each model is developed.

4. LOAD MODELLING

In recent years, interest in load modelling has considerably increased because it has been proven to significantly influence power system analysis, planning and control. Thus, the need for developing new load models or updating existing ones towards serving the needs of the continuously changing power systems in Europe and worldwide is imperative [1]. Load models often fail to incorporate socio-technical factors as well to address how, specifically, occupants consume energy in their homes; in real-time; based on their individual preferences [2]. To this end, multidisciplinary and dynamic approaches should be adopted to enhance energy efficiency without compromising comfort and individual needs and preferences.

To this end, load modelling has been the subject of many modern studies as a prerequisite for the mitigation of high renewable integration, as demand-side management enabler leveraging the increasing penetration of smart metering devices in the current energy systems. However, there is a need to systematically review existing load modelling techniques and suggest future research directions to meet the growing interests from industry and academia. To this end, in the following section, we will present a brief description of load models and parameter identification methods found in the literature, before the FLEXCoop approach and the respective DER load models to be presented and analysed. The literature review is primarily based on a recently published article by Ammar Arif et al. in the IEEE Transactions on Smart Grids [1].

4.1. Load Modelling Approaches – Literature review

Considering that FLEXCoop aims at utilising the aggregated flexibility provided by residential consumers, in what follows we will limit our analysis to the description of the models found in the literature that approximate the behaviour of Low Voltage (LV) residential loads. Therefore, from this point forward, by using the term “loads” we will strictly refer to LV residential loads.

In general, there are two approaches commonly used in modelling residential energy consumption [2]:

- the **top-down approach** that treats the loads as an energy sink and is not concerned with individual end-uses. The strength of this approach is that it only needs aggregated data that are commonly and easily available. However, its strength is also its weakness because it does not take into account the individual end-users, consumers’ comfort and preferences. Thus, it is inappropriate for the establishment of a holistic human-centric framework, which is the key target aim of the FLEXCoop project;
- the **bottom-up approach** that identifies the contribution of each end-use towards aggregating energy consumption. Input data that are commonly used in such models include: dwelling characteristics, indoor and outdoor environmental conditions, occupancy patterns, specific equipment used, etc. This approach can accommodate user preferences and individual energy consumption; thus, it is in line with the FLEXCoop objective, which focuses primarily on the consumer himself/herself, his/her needs, comfort and preferences.

  Both *statistical* (e.g. regression, conditional demand analysis, neural network) and *engineering* (e.g. distributions, archetypes, sample) methods are used in the literature for the bottom-up modelling of the energy consumption of individual end-users [2]. The detailed description of these models is out of the scope of this deliverable and thus, they are not further analysed. More detailed information, however, can be found in [2].

The most important strength of the bottom-up statistical models, from the FLEXCoop point of view, is that they encompass occupant behaviour. This fact played a decisive role in the design of the FLEXCoop DER load models presented below.

4.2. Load Model Parameter Identification – Literature Review

There are two basic methods that are most frequently used for the identification of the load model parameters [1]. Both of them can be used in a bottom-up approach modelling, described in the previous section.

- The **component-based approach** needs the following datasets in order to be structured: (i) the models of individual components and (ii) the composition of the individual components, meaning the percentage of load consumed in each component. This approach requires accurate and comprehensive load composition information that is frequently very hard to obtain. Additionally, its low adaptability to new loads makes it impractical for a holistic framework like the one that FLEXCoop introduces.
- The **measurement-based approach** is implemented in four (4) phases: (i) obtain measurement data; (ii) select a load model structure (e.g. polynomial); (iii) estimate model parameters; (iv) validate the load model. This approach can be used to reflect real-time dynamic load behaviours and thus, it could be a favourable solution to be adopted in FLEXCoop. Among others, least-square methods have been widely used for the identification of model parameters in the frame of the measurement-based approach. This is adopted also in FLEXCoop and thus, it is further detailed below.

4.3. The FLEXCoop Load Modelling Approach

Having presented an overview of the different approaches used for the modelling of the residential loads, we now proceed to the identification of the specific FLEXCoop requirements that should be satisfied by the DER load modelling. This section is of high importance because it presents all the information that have practically guided us in the selection of the most appropriate approaches and relevant models towards achieving the overall FLEXCoop scope [3]:

"***To provide innovative services that will be featured by non-intrusiveness, comfort and well-being preservation and non-violation of each individual prosumer daily schedule***".

Thus, in this section, we will present the proposed FLEXCoop DER load device models along with the relevant processes required to define and formalise their control and response capabilities towards defining their flexibility capacity in DR programmes. The scope of the FLEXCoop load modelling is to establish a holistic approach that takes into account demand capabilities to participate in various DR strategies. The DER load models will subsequently be combined with user comfort profiles (as they will be defined in task T3.2) to produce energy demand models. The enhanced robust and dynamic energy demand models will incorporate the comfort flexibility of users (e.g. comfortable ambient condition ranges) leading eventually to a model/profile of the energy demand flexibility for the specific load. For instance, tolerable temperature variations in the building can be translated into energy demand flexibility of the HVAC system. The holistic context-aware flexibility profiling models will also be delivered in the task T3.2.The FLEXCoop DER load models correlate mathematically with the electric

demand of each DER type to various parameters including the existing (indoor/outdoor) environmental conditions and the operational data of DER load devices. The proposed models are described in detail in the following subsections. All of the DER load models have been constructed in a way that ensures the fulfilment of FLEXCoop objectives and business requirements. More specifically, the models should:

- refer to residential loads with significant capacity to affect the building-level energy demand and provide flexibility as well as support the indoor environment optimisation in terms of comfort and health preservation. To this end, ***Heating, Ventilation and Air Condition (HVAC)*** and ***lighting*** have been identified as the most suitable loads and thus are further elaborated below;
- encompass ***occupant behaviour***;
- be based on ***simple mathematical formulas*** that can approximate load behaviours minimising complexity to the degree possible;
- provide relatively ***reliable results*** enabling the accurate forecasting of DR potential and demand flexibility in the short and very short term. Short-term forecasting will cover the 24h ahead and will deliver predicted values in periods of 1h. Very short-term forecasting will cover periods from 4 hours ahead to, even, 1 hour prior to a DR event to enable decision making optimization (for the flexibility that needs to be activated) on the aggregator side;
- be ***beneficial*** for the consumers in both financial and comfort terms ensuring their sustainable participation in automated DR strategies on the basis of aggregated flexibility utilisation;

From the above requirements combined with the description provided in 4.1 and 4.2, it is easily deduced that FLEXCoop business and technical requirements will be satisfied through the use of ***bottom-up statistical*** models combined with a ***measurement-based approach*** for the learning process. The learning process is actually the process of identifying each model's parameters. This is further elaborated in each DER model type analysed below i.e. lighting and HVAC. Although the learning process will be common for the models of the same type of DER loads, the model parameters that will be extracted through this process will be uniquely identified for each specific pilot dwelling during the implementation and deployment of the FLEXCoop solution. Furthermore, the FLEXCoop modelling framework will allow for continuous calibration of the respective DER models in order to account for efficient and effective dynamic adaptation to potential shifts in the "behaviour" of the corresponding physical entities (seasonal patterns, device performance degradation, etc).

FLEXCoop Load Models

As already mentioned, the FLEXCoop DER load models contain the mathematical formulas for the calculation of electric demand (consumption) of each DER type as a function of dynamic (input data) and static (configuration) parameters affecting DER operation.

A training period, gathering data from the physical devices is required towards the extraction of the modelling parameters. By having defined these parameters following a learning process:

1) model parameters can be periodically updated by taking into account recent data and

2) enhanced real-time DER instances can be provided (by considering the input and configuration parameters, as defined in the following sections), further facilitating the DER operation simulation under different environmental/contextual conditions.

In the following subsections, we detail the lighting and HVAC models along with the respective input, output and configuration parameters. The DER models presented below were constructed respecting all the FLEXCoop requirements defined above.

4.4. Lighting Devices

4.4.1. DER model

An important aspect that is exploited in FLEXCoop considering lighting devices is that the dimming level and energy consumption in lighting systems is directly correlated without any delays or memory effects. This enables the immediate and controllable modification of the energy consumption of a lighting system.

Herein, we assume a simplified case where a lighting device or a number of lighting devices are installed in a room with common control. Then, the light device model can be defined as: "power consumption as a function of status and dimming level". Therefore, the learning model is based on the definition of the average consumption values for the different device status (on/off) and dimming levels (0-100%).

The lighting device instantaneous power consumption can be approximated by the following mathematical formula:

$$P_{output} = Nominal_{Power} \cdot Status \cdot Dimming_{level} \rightarrow$$
$$P_{output} = \begin{cases} 0, & when\ Status = 0\ (Off) \\ Nominal_{Power} \cdot Dimming_{level}, & when\ Status = 1\ (On) \end{cases} \quad (1)$$

Where $\boldsymbol{P_{output}}$ is the light load consumption and $\boldsymbol{Nominal_{Power}}$ is the nominal power of the lighting system. $\boldsymbol{Nominal_{Power}}$ is the configuration parameter in this equation and is extracted through a measurement-based learning process that is described below. A regression analysis can be performed to correlate input (dimming level and device status) and output (consumption) values towards identifying the configuration factor ($\boldsymbol{Nominal_{Power}}$).

> *"In statistical modelling, regression analysis is a set of statistical processes for estimating the relationships among variables. It includes many techniques for modelling and analysing several variables, when the focus is on the relationship between a dependent variable and one or more independent variables (or 'predictors'). More specifically, regression analysis helps one understand how the typical value of the dependent variable (or 'criterion variable') changes when any one of the independent variables is varied, while the other independent variables are held fixed."*
>
> *Wikipedia [4]*

Linear regression is a basic and commonly used type of predictive analysis. It attempts to model the relationship between two variables by fitting a linear equation to observed data. One variable is considered to be an explanatory variable, and the other is considered to be a dependent variable. A linear regression line has an equation of the form $\boldsymbol{Y = a \cdot X + b}$, where X is the explanatory variable and Y is the dependent variable. The slope of the line is $\boldsymbol{a}$, and $\boldsymbol{b}$ is the intercept (the value of $\boldsymbol{Y}$ when $\boldsymbol{X}$ =0).

The most common method for fitting a regression line is the method of least-squares. This method calculates the best-fitting line for the observed data by minimizing the sum of the squares of the vertical deviations from each data point to the line (if a point lies on the fitted line exactly, then its vertical deviation is 0). Therefore, given a random sample from the population, we estimate the population parameters and obtain the sample linear regression model.

Once a regression model has been fit to a group of data, examination of the residuals (the deviations from the fitted line to the observed values) allows the modeller to investigate the validity of assumption that a linear relationship exists. Plotting the residuals on the y-axis against the explanatory variable on the x-axis reveals any possible non-linear relationship among the variables.

For the lighting devices, the slope parameter $\boldsymbol{a}$ is the $\boldsymbol{Nominal_{Power}}$ factor, as it is deduced from equation (1) in case of the status device being on (i.e. $\boldsymbol{Status = 1}$). In general, for a LED luminaire light (which we expect to be the case for the FLEXCoop pilot end users), there is a fairly linear dependence between the luminaire input power and the emitted visible light (luminous flux measured in lumens – lm)**[5]**. Furthermore, the amount of luminous flux falling on a surface due to an isotropic light source is directly proportional to the intensity of the light source. Thus, again a linear regression analysis can be a relatively good approximation and it can be performed at an initial stage. If significant non-linearities are observed, the model will be re-constructed accordingly. However, we expect that a linear behaviour could provide results accurate enough for its incorporation to the FLEXCoop holistic context-aware profiling mechanism.

Thus, by performing linear regression analysis, we can easily identify the slope parameters $Nominal_{Power}$. Having this configuration parameter defined, we can easily estimate consumption for different light device statuses and dimming levels. However, a fully automation process must take into account the real-time environmental conditions and user preferences, so it is critical to calibrate our model. To this end, it is necessary to identify the lighting devices' impact on the illuminance measured by the relevant sensor(s) and associate this with the illuminance actually detected and experienced by the occupant(s). Of course, the latter may greatly vary amongst people because it is strongly defined by individual preferences including parameters that cannot be straightforwardly measured (e.g. psychological). To this end, this correlation should be considered in two steps:

(i) Correlation of the lighting device (artificial light) impact on the measured illuminance value at the sensor with the respective impact at the illuminance value at a specific area in the house where the occupant exists (e.g. a defined zone at the workplace plane);
(ii) Correlation of the illuminance value at a specific area in the house where the occupant exists with the illuminance preferred by the occupant. This is the subject of the task T3.2 concerning comfort profiling and will be further described in the corresponding deliverable D3.2.

The idea behind the calibration and configuration of the proposed model towards addressing these requirements is detailed in the sub-section below.

4.4.2. DER model calibration and definition of daylight contribution

As mentioned above, there are two aspects that should be covered (if we analyse further the step (i) presented above):

- Definition of artificial light / daylight impact on the illuminance measured by the installed sensor(s);
- Definition of the relationship between the measured illuminance value at the light sensor(s) and the average illuminance value at a specific area where the occupant(s) stay(s). For simplicity reasons, we will consider one occupant in a room office in a specific zone of the workplace plane. However, we recognise the fact that depending on the type of the room and its actual use, another area may be more appropriate to be used for calibration purposes. This will be further examined after the selection of the final pilot end-users.

Caicedo et al.**[6]** have proposed a framework for the disaggregation of illuminance levels on ambient luminance and luminance contribution from lighting devices towards providing a daylight-adaptive lighting control system. Based on this study, we present a simplified approach considering a lighting system in an indoor office, with N light sources and one luminance sensor at the ceiling. This is considered to be closer to the actual installation that we currently expect to deal with in the real FLEXCoop pilot users. This will be further evaluated after the pilot surveys in the selected pilot users and the equations presented below will be reconfigured accordingly ensuring the provision of accurate and reliable results that can fulfil the real-life needs.

The average net illuminance $\boldsymbol{w(d,u)}$ at the specific zone at a given time t, given that the lighting system is at dimming vector d ($|\boldsymbol{d}| = \boldsymbol{Dimming_{level}}$[3]), may be written as:

$$w(d,u) = \sum_{n=1}^{N} H_n d_n + u \tag{2}$$

Where $\sum_{n=1}^{N} \boldsymbol{H_n d_n}$ and $\boldsymbol{u}$ is the illuminance contributions due to lighting system and daylight at the specific defined zone respectively, as shown in Figure 4. $\boldsymbol{H_n > 0}$ is the illuminance contribution to the average on the defined zone when the nth light source is at maximum intensity, with all the other light sources turned off.

[3] The $Dimming_{level}$ that was defined in Section 4.4.1 is the magnitude of the dimming vector d (i.e. $Dimming_{level} = |d|$) shown in Figure 4.

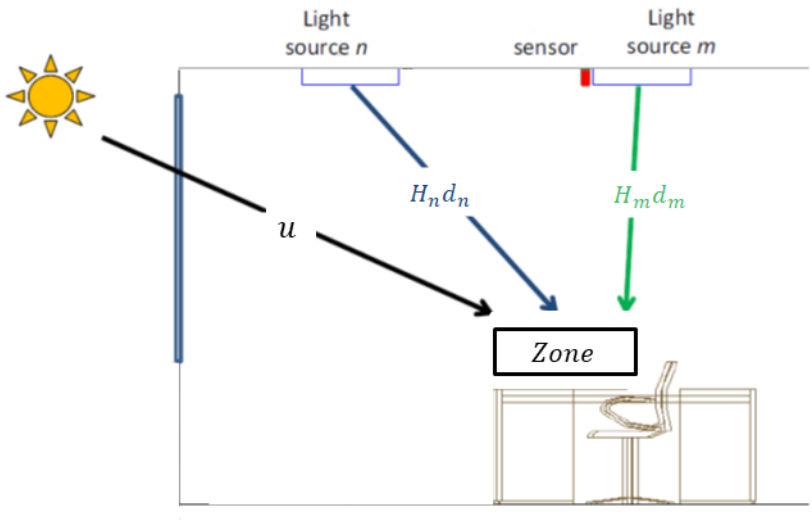

Figure 4: Average illuminance at a specific zone at the workspace plane due to artificial light and daylight (re-design of the figure provided in **[6]**)

In most of the installation cases where light sensors are installed on the ceiling, illuminance values at specific zones cannot be measured; only illuminance measurements at the light sensor are available following the sensor installation as depicted in the illustration above (ceiling installation).

Therefore, the measured illuminance at a light sensor in the ceiling is the net illuminance due to contributing light sources and daylight reflected from the objects (e.g. furniture) in the office. Denote $\boldsymbol{E_n}$ the measured illuminance at the light sensor when the nth light source is at maximum intensity, in the absence of daylight. We assume that the illuminance scales linearly with the dimming level. This assumption holds well for practical light sources, e.g. LED light sources. The instantaneous net illuminance at the sensor at the ceiling, given that the lighting system is at dimming vector $\boldsymbol{d}$ and under daylight, can then be written as:

$$\boldsymbol{I(d,s)} = \sum_{\boldsymbol{n=1}}^{\boldsymbol{N}} \boldsymbol{E_n d_n} + \boldsymbol{s} \tag{3}$$

Where $\sum_{n=1}^{N} \boldsymbol{E_n d_n}$ is the illuminance due to the lighting system and $\boldsymbol{s}$ is the illuminance due to daylight measured at the sensor, as it is illustrated in Figure 5.

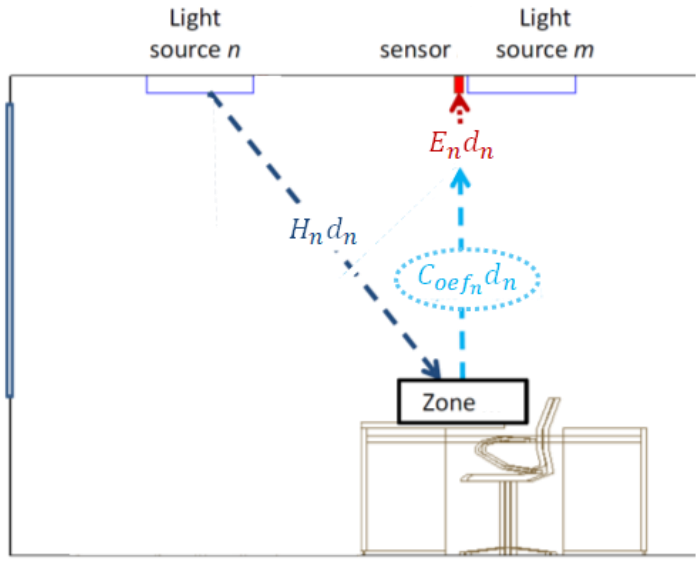

Figure 5: Illuminance contribution at the light sensor due to the artificial light (with absence of daylight) from light source n reflected from the defined zone (re-design of the figure provided in **[6]**)

In practice, the $\boldsymbol{E_n}$ values may be computed a priori in a calibration phase by turning on the light sources to the maximum intensity one at a time and measuring illuminance values at the light sensor in the absence of daylight. Further, we can relate the average illuminance values at the specific zone and illuminance values at the light sensor at a given time t by:

$$\sum_{n=1}^{N} E_n d_n = \sum_{n=1}^{N} G^{(n)} H_n d_n \tag{4}$$

$$s = G^{(0)} u \tag{5}$$

Where $\boldsymbol{G^{(n)} > 0}$ is the illuminance contribution at the light sensor when the average illuminance at the defined zone due to the nth light source is at the maximum and $\boldsymbol{G^{(0)} > 0}$ is the illuminance contribution at the light sensor when the average illuminance at the defined zone due to daylight is $\boldsymbol{u}$ (see Figure 6).

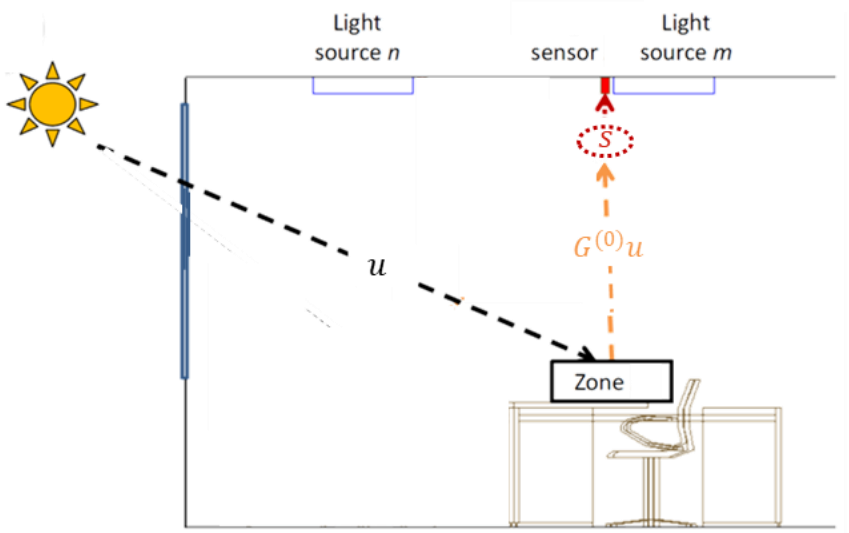

Figure 6: Illuminance contribution at the light sensor due to daylight (with absence of artificial light) reflected from the defined zone (re-design of the figure provided in **[6]**)

Through analytics over historical data (illuminance values and dimming levels) the $\boldsymbol{G^{(n)}H_n}$ factors are calculated for n=1, …, N. This is the $\boldsymbol{C_{oef_n} = G^{(n)}H_n}$ (practically equal to the $\boldsymbol{E_n}$ parameter) for each lighting device, presented in the model section above (equation (4)), expressing the impact context parameter of a specific lighting device on the measured illuminance level by the light sensor. Then, the external illuminance level impact at given time t is calculated by equation (3) as follows:

$$\boldsymbol{s = I(d, s) - \sum_{n=1}^{N} C_{oef_n} d_n} \quad (3)$$

This information can be exploited afterwards during the optimisation process towards obtaining the dimming vector that minimises the power consumption of the artificial lighting based on the net illuminance values measured by a light sensor.

It should be pointed out at here that in FLEXCoop project, the illuminance sensor topology will be selected taking into account the specific topology of each pilot dwelling combined with the potential budget constraints implied by the project. For example, it is possible to install just one illuminance sensor in a fixed position, however appropriately selected to monitor specific spaces in each pilot dwelling. This may induce implications compared to a multiple sensor topology or sensors that are positioned in the comfort bubbles of the occupants. To this end, the calibration process described herein will be a dynamic process and the relevant parameters will be continuously updated based on user preferences/ profiling data. This, will allow us, even if we need to use simplified sensor topologies, to be able to account for daylight seasonal patterns as well as changes in space topology.

4.4.3. DER model parameters

Summing up, the FLEXCoop lighting DER model parameters are estimated by:

1) calculating the power profile as a function of status/dimming level of each different light device (equation (1));
2) estimating the C_{oef} or H_n parameters of each lighting device i.e. contribution of each light (or group of lights) to the dedicated zone (comfort bubble). E.g. in a topology where the illuminance sensor will be placed inside an appropriately selected zone and not on the ceiling, the H parameter(s) can be easily extracted by a linear regression analysis as follows:

$$Sensor_{value} = \sum_{n=1}^{N} H_n d_n$$

   These values can be easily calibrated for each specific lighting device by turning off all the lighting devices of the examined area except for the one whose H is going to be extracted, in the absence of daylight.
3) estimating the daylight contribution to the dedicated zone (comfort bubble) illuminance levels.

The table below summarises the lighting DER model parameters (input/ configuration/ output) presented above.

Table 1: Light Device DER Model Parameters (defined per lighting device installed in the examined area)

PARAMETER	DESCRIPTION	UNITS	TYPE
Configuration Parameters			
$Nominal_{Power}$	Nominal power of the lighting device	W	Float
C_{oef}	Impact of the lighting device on the illuminance value measured by the light sensor (for a sensor placed at the ceiling)	Lux	Float
H	Illuminance contribution to the average on the defined zone when the specific light source is at maximum intensity (for a sensor placed at a dedicated zone), with all the other light sources turned off	Lux	Float
Input Parameters			
$H_{preferred}$	Preferred illuminance value at a dedicated zone[4]	Lux	Float

[4] This combines the actual illuminance level at the dedicated zone with the visual comfort profiles that are examined in the T3.2.

PARAMETER	DESCRIPTION	UNITS	TYPE
Output Parameters			
$Dimming_{level}$	Percentage of the brightness provided by the lighting device	%	Float
P_{output}	Estimated power consumption of the lighting device for the defined $Dimming_{level}$	W	Float

4.5. HVAC Devices

The load type with the highest potential for DR programs is electric powered HVAC. There are electric options that provide heating and cooling as well as heating-only and cooling-only options. A variety of heating and cooling technologies combined with different ventilation strategies are successfully being applied. Individual, centralised and district/collective solutions are encountered in Europe and worldwide. However, only the individual solutions fall into the FLEXCoop scope and thus, in what follows, we limit our analysis and modelling approach to ***individual electric HVAC solutions***[5]. This may include air-to-air heat pump, air-to-water heat pumps, air conditioners (ductless mini-split units), electric resistance heaters, hybrid systems, electric boilers, etc.

A recently published report of the Stratego project [7] summarizes data considering the relative distribution of electrical heat demand in terms of heat pumps and other electric heating systems throughout the EU28 Member States. Based on this report [8], 82% of electrical heat demand of the residential sector in Netherlands comes from heat pumps. The corresponding percentage in Spain is 25%, much lower but still significant. These data[6] combined with our survey and analysis performed so far (albeit still in progress) regarding the potential FLEXCoop pilot users led us to incorporate in our modelling the following electric powered HVAC systems:

- ***Heat pumps*** (air-to-air and air-to-water)
- ***Air conditioners*** (air/air ductless mini-split units)

The main principles of operation, the assumptions that need to be made and the proposed models are detailed in the following sub-sections.

Having these models, we will then need to develop new ones towards correlating the HVAC device status (mode, set-point) and environmental/contextual conditions (e.g. ambient temperature) to the heat demand and thus to the electrical energy consumed. However, this

[5] Individual HVAC solution is considered the system that its control affects only one user or group of users living in the same dwelling.

[6] We only consider data for the Netherlands and Spain, because FLEXCoop pilot end-users are located in these countries.

requires also the thermal zone modelling that will be developed and analysed in the Task 3.3 as well as the comport profiling models that will be delivered in the Task 3.2.

Heat pump Operating Principle

In principle, the operation of most heat pumps is based on the vapor-compression cycle depicted in Figure **7**, which exploits the physical properties of a volatile evaporating and condensing fluid (so-called refrigerant) and the heat stored or released during its phase change. The main components of a heat pump are: a compressor, an expansion valve and two heat exchangers namely the evaporator and the condenser (also shown in Figure **7**).

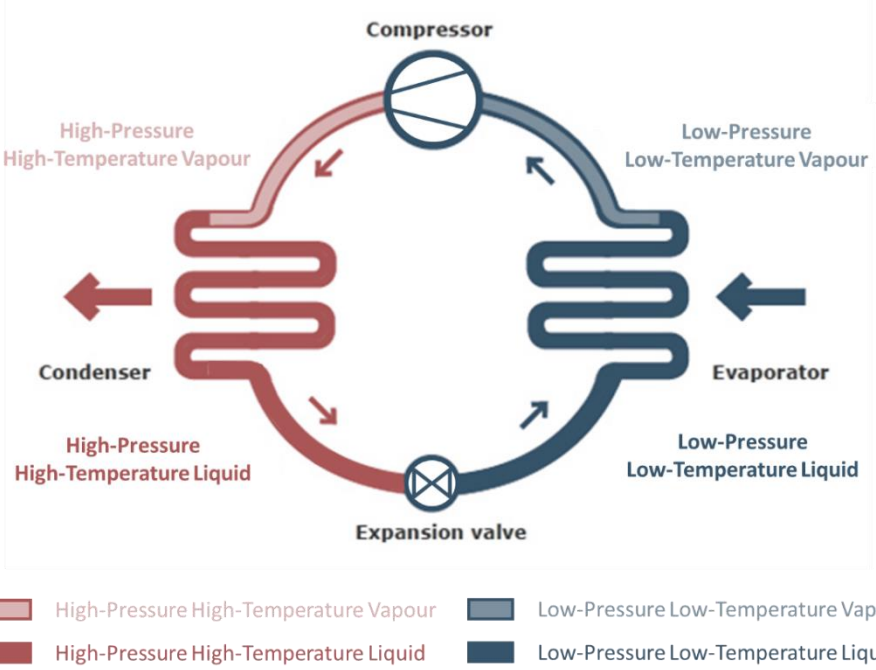

Figure 7: Vapour compression cycle

In heating mode, the cycle starts with the liquid refrigerant exiting the condenser. Then, it passes through the expansion valve, which reduces its pressure. The low-pressure liquid passes through the evaporator absorbing heat from a source (e.g. outdoor air for the air sourced heat pumps that will be examined in FLEXCoop) and is evaporated. The low-temperature vapour is then compressed to a higher pressure raising its temperature (when passing through the compressor). On the discharge side of the compressor, the now hot and highly pressurized vapour passes through a heat exchanger, called condenser, until it condenses again (phase change because it rejects heat through a heat sink) into a high pressure and temperature liquid. It is critical that the refrigerant reaches a sufficiently high temperature when compressed to release heat through the condenser. The heat can be released inside the dedicated building either as warm air (air-to-air heat pump) or as hot water-filled radiators, underfloor heating and/or domestic hot water supply (air-to-water heat pumps).

Air conditioner (ductless mini-split system) operating principle

Ductless mini-split air-conditioners rely also on a vapour compression cycle (see Figure **7**) to transfer heat, similar to conventional heat pumps. Their difference is found on the way the conditioned air is supplied to the home. Conventional split-system heat pumps have one indoor

coil in an air-handling unit and use forced-air distribution through ductwork to deliver conditioned air to various zones within a home. In contrast, ductless mini-splits connect one or more indoor coils (often referred to as "heads" or "fan coils") to a single outdoor unit (i.e., the condenser), with each head having its own refrigerant loop. Conditioned air is provided directly to the rooms in which the heads are located, without the use of ductwork. Mini-split systems with more than one indoor head (sometimes referred to as "multi-split" systems) enable specific zones to be conditioned independently because each indoor unit has its own thermostat [9].

4.5.1. HVAC DER model

4.5.1.1. Heat pump DER model

The modelling of a heat pump is primarily based on the estimation and relationship of electrical consumption and heat released to a dedicated ***thermal zone***. The thermal zone definition is provided below.

> *"Thermal zone stands for independent parts of the building, characterized by the different usage made, HVAC or electrical facilities, with different criteria of usage or with independent indoor environmental control systems and management."*
>
> *Green Energy Audit of Buildings [10]*

From the above definition, it is clearly deduced that the selection of thermal zones in the pilot sites will strongly depend on the specific building characteristics, available equipment and usage patterns. An in-depth analysis will be performed in the end-users' dwellings to define the most appropriate thermal zones. To do so, input from Task 3.3 on thermal modelling of buildings is also required. We will not get into more detail on this subject here because it is out-of-the scope of the deliverable. However, a comprehensive analysis will be performed both in T3.3 and in the pilot survey in T7.1 that will be efficiently combined to ensure that reliable results, to the degree possible, will be obtained through the HVAC modelling proposed below. Of course, these models may be adapted, enhanced and/or re-configured as the project progresses to meet specific requirements identified throughout its implementation and deployment.

The instantaneous efficiency or Coefficient Of Performance (COP) of a heat pump is defined as the ratio of the thermal power delivered to a thermal zone by the heat pump ($\dot{Q}_{hp}$) to the electrical power consumed (P_{el}):

$$\mathrm{COP} = \frac{\dot{\mathrm{Q}}_{hp}}{\mathrm{P}_{el}} \tag{6}$$

A simplified illustration of electrical and heat flows taking place during heat pump operation is shown in Figure **8**. More specifically, $\dot{\mathrm{Q}}_{\mathrm{hp}}$ is the thermal power delivered to the thermal zone from the heat pump at the condenser side (see Figure **7**), P_{el} is the electric power consumed by the heat pump and $\dot{\mathrm{Q}}_{\mathrm{C}}$ is the thermal power extracted from the ambient air at the evaporator side (see Figure 7).

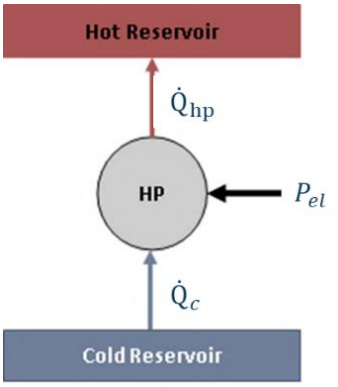

Figure 8: Heat pump model

The estimation of the COP enables us to transform consumed electrical energy to supplied thermal energy of the heat pump and vice versa. A significant complication arises from the fact that, depending on the heat pump type, the supplied thermal power and COP depend on multitude parameters as for example the outlet medium temperature and the ambient temperature (for air sources). This can be expressed mathematically as follows:

$$\dot{Q}_{hp} = f(T_{amb}, T_{HP,out}) \quad (7)$$

$$COP \sim f(T_{amb}, T_{HP,out}) \quad (8)$$

Where T_{amb} is the outdoor ambient temperature and $T_{HP,out}$ is the output temperature of the heat pump's transfer fluid. In the ideal case of zero losses and by using the efficiency definition from Carnot cycle:

$$P_{el} = \dot{Q}_{hp} - \dot{Q}_C \quad (9)$$

$$COP_{Carnot} = \frac{T_{HP,out}}{T_{HP,out} - T_{amb}} \quad (10)$$

However, in real life the COP of a heat pump is much lower than the one predicted by the Carnot cycle. Many researchers have dealt with these issue and have estimated the actual COP of heat pumps based on detailed mathematical models [11], [12]. However, these models are very complex based on highly non-linear functions that in turn require high computational power to be solved. This is not aligned with the FLEXCoop requirements presented in Section 4.3. An alternative has been proposed by other authors representing heat pumps by polynomial fitting of experimental results [13], [14]. This latter approach will be adopted also in FLEXCoop. The proposed polynomial functions and the assumptions standing behind them are described in the following paragraphs in different proposed scenarios.

As indicated above, the COP is mainly a complex function of the output temperature $T_{HP,out}$ and outdoor temperature T_{amb}. We can assume negligible secondary effects such as partial loads (i.e. effect of compressor frequency *f* on the P_{el}) and humidity, which indeed have only minor effects in COP compared to its dependency on the two temperature values defined above. Therefore, the approximation shown in equation (8) can be assumed accurate enough for the scope of the modelling required by the FLEXCoop project.

Scenario A

According to POLIMI [15], it is possible to get a very good approximation of the COP by fitting a third order polynomial function to experimental data, as follows:

$$\mathrm{COP} = \mathrm{COP}_0 - \mathrm{a}_0\mathrm{T}_{\mathrm{HP,out}} + \mathrm{a}_1\mathrm{T}_{\mathrm{HP,out}} - \mathrm{a}_2\mathrm{T}_{\mathrm{HP,out}}^2 - \mathrm{a}_3\mathrm{T}_{\mathrm{HP,out}}\mathrm{T}_{\mathrm{amb}} + \mathrm{a}_4\mathrm{T}_{\mathrm{amb}}^2 - \mathrm{a}_5\mathrm{T}_{\mathrm{amb}}^3 - \mathrm{a}_6\mathrm{T}_{\mathrm{HP,out}}^3 \quad (11)$$

The COP_0 is the reference value for the COP and $\mathrm{a_i}$ are constant interpolating coefficients. These can be calculated using e.g. least square fitting, as presented in Section 4.4.1.

Figure 9 presents a validation experiment on a reference heat pump performed by POLIMI [15]. The figure shows the interpolated COP in green and the measured COP in red with respect to the supply temperature $\mathrm{T_{HP,out}}$ and the environment temperature $\mathrm{T_{amb}}$.

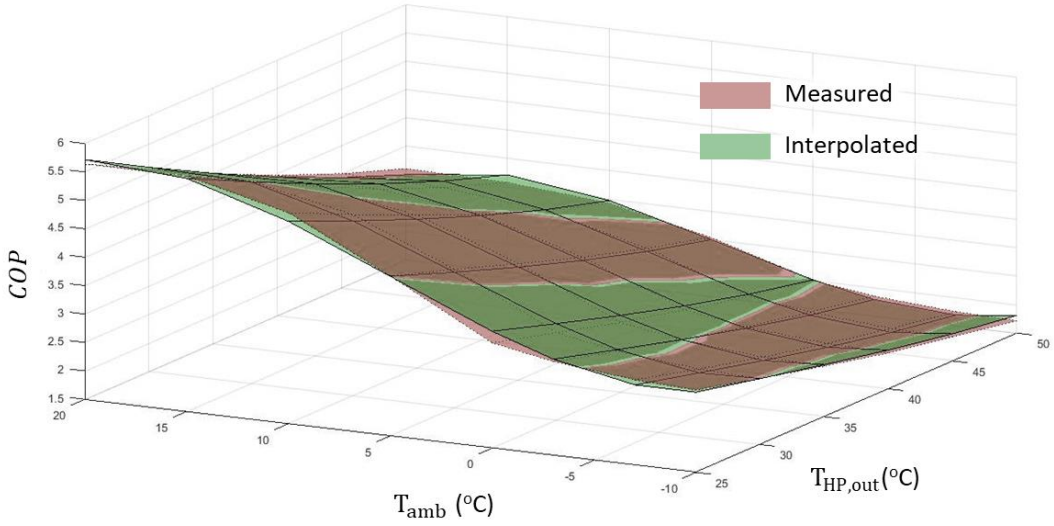

Figure 9: Example estimated vs. actual COP of a reference heat pump using a third order polynomial to model the HP performance

As clearly shown in Figure 9, there is a very good agreement between the estimated COP values and the experimental ones for the whole range of temperature examined. However, this approach will lead to a highly nonlinear formulation for the control optimization formulations that need to be performed later on. Thus, despite its proven accuracy, this approach will not be further examined in the project.

Scenario B

In this scenario the dependency of the COP on $\mathrm{T_{amb}}$ and $\mathrm{T_{HP,out}}$ is taken into account by a quadratic fit in these two variables. In particular, the COP is represented by the following 2nd order polynomial function:

$$\mathrm{COP} = COP_0 + c_1 T_{amb} + c_2 T_{\mathrm{HP,out}} + c_3 T_{\mathrm{HP,out}}^2 + c_4 T_{\mathrm{amb}}^2 + c_5 T_{amb} T_{\mathrm{HP,out}} \quad (12)$$

The COP_0 is again the reference value for the COP and $\mathrm{c_i}$ are the constant interpolating coefficients.

This approach has been validated at standard and non-standard (analysis far from typical catalogue data) conditions by D. Carbonell et al. in [16]. In this work, the authors concluded that by fitting experimental data to a 2nd order polynomial equation (to obtain the constant interpolating coefficients of equation (12)), the model can predict actual measured COP. The

model provides very satisfactory results with error less than 5% at standard conditions and less than 15% at non-standard conditions, as illustrated in Figure **10**.

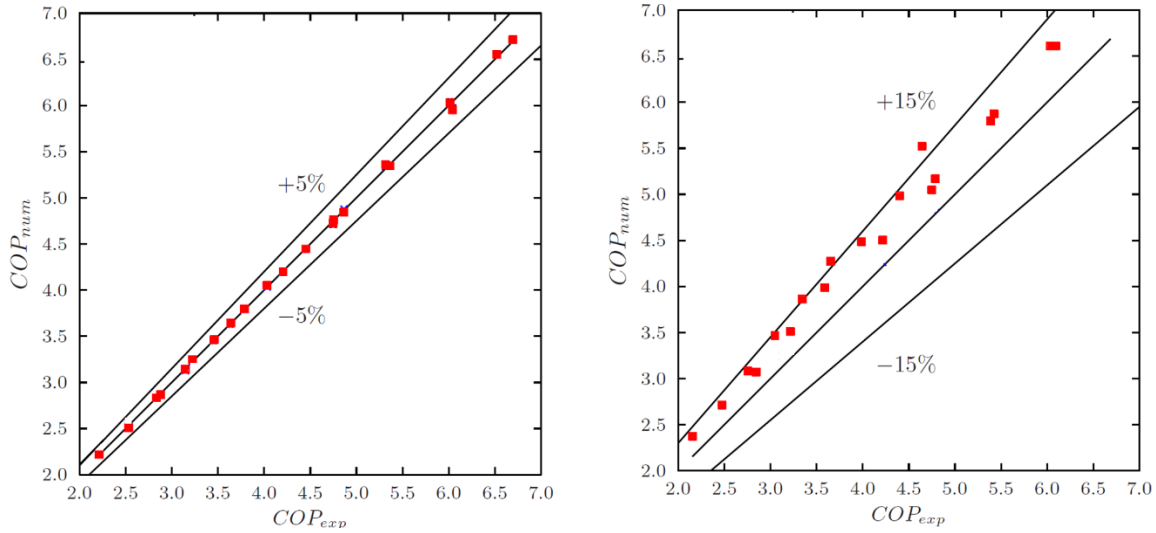

(a) (b)

Figure 10: Numerical results of estimated COP compared with experimental results for: (a) standard and (b) non-standard conditions **[16]**.

Scenario C

This scenario simplifies further the heat pump model considering $T_{\mathrm{HP,out}}$ as a constant. Although $T_{\mathrm{HP,out}}$ is assumed as a constant, it can be updated for each new iteration towards providing more accurate results. Therefore, in this simplified scenario, COP can be expressed as $\mathrm{COP}\sim f(\overline{T_{\mathrm{HP,out}}}, \mathrm{T_{amb}})$. $\mathrm{T_{amb}}$ can further be assumed as a known value based on the predicted environmental temperature obtained from weather data. This way, COP is a known value for each time step, so that the optimization function that will need to be solved during optimisation process can be approximated by a linear function of $\dot{Q}_{hp}$ considering that:

$$\mathrm{P_{el}} = \frac{\dot{\mathrm{Q}}_{\mathrm{hp}}}{COP(\overline{T_{\mathrm{HP,out}}}, \mathrm{T_{amb}})} \tag{13}$$

Scenario D

This scenario neglects also the dependency of COP on the $\mathrm{T_{amb}}$ and thus, it is considered as a constant for the entire horizon ($COP\sim Const$). This results in a constant ratio of $\dot{\mathrm{Q}}_{\mathrm{hp}}$ and $\mathrm{P_{el}}$ expressed as follows:

$$\mathrm{P_{el}} = \frac{\dot{\mathrm{Q}}_{\mathrm{hp}}}{Const} \tag{14}$$

The constant value of COP can be found using equation (12) with the daily mean ambient $\mathrm{T_{amb}}$ and the corresponding steady state value for $T_{\mathrm{HP,out}}$ [14].

It should be mentioned here that the overall objective of the HVAC modelling in FLEXCoop is to optimise the heat pump operation towards participating in FLEXCoop DR strategies respecting occupants' thermal comfort. These may be conflicting and correlated objectives and the optimisation framework that will be developed as the project progresses (in the tasks T3.5

and T5.3) should assess the currently presented models towards utilising the most appropriate one that will result in an optimal solution based on the different requirements and constraints.

4.5.1.2. Air conditioner (ductless mini-split system) DER model

Based on the operating principle described in the previous section, it is easily deduced that the modelling approach of the air conditioning system is akin to the model of a heat pump. The only difference between the two models is that the air condition system releases the heat / takes up the heat directly from the air, i.e. from the building model. The heat generated is dependent on the ambient and indoor room temperature based on a performance map look-up.

Again, the model may be elaborated further to accommodate any requirements introduced by the optimisation framework that will be adopted.

4.5.2. DER model calibration

Each of the HVAC DER models that will be selected for use in the FLEXCoop demonstration purposes will be calibrated based on the exact equipment installed in the final pilot users, hence avoiding a "one-size-fit-all" solution that would yield non-negligible errors. Well-calibrated models will be provided to enable an accurate enough formulation of the HVAC systems found in pilot dwellings. The specific installation types will also be taken into account in the calibration process towards enabling the better representation of each specific HVAC system by the most appropriate DER model.

4.5.3. DER model parameters

The table below summarises the HVAC model parameters (input / configuration / output) presented above.

Table 2: HVAC Device DER Model Parameters (defined per dedicated thermal zone)

PARAMETER	DESCRIPTION	UNITS	TYPE
Configuration Parameters			
Constant interpolating parameters (Only for scenarios A, B and C)	The constant parameters that need to be defined by fitting data to the polynomial functions defined in the different scenarios	Vary depending on the constant	Float
COP (Only for the scenario D)	Coefficient of performance of the HVAC system	--	Float
Input Parameters			

PARAMETER	DESCRIPTION	UNITS	TYPE
Type	Heat Pump, AC (ductless mini-split system)	--	String
T_{amb}	Ambient Temperature	K	Float
$T_{HP,out}$ (Only for the scenarios A, B and C)	Output temperature of the heat pump's transfer fluid	K	Float
$\dot{Q}_{hp}$	Thermal power needed to be delivered to a thermal zone by the HVAC system (This value should be provided by the thermal zone modelling combined with comfort profiling, which are the subjects of the T3.3 and T3.2 respectively)	W	Float
Output Parameters			
COP (Only for the Scenarios A, B and C)	Coefficient of performance of the HVAC system	--	Float
P_{el}	Power that will be consumed by the HVAC system to cover the required heat demand	W	Float

5. STORAGE MODELLING

Electric energy storage devices are basic components in the smart grid framework – the electric system of the future. Following this idea, Energy Storage Systems (ESS) are important components in the FLEXCoop project. This importance can be derived from business scenarios analysed in the project (as identified in the D2.1). For the following business scenarios of the FLEXCoop project, ESS is essential for:

2. Consumption optimization of cooperatives resources

    2. a. Self-consumption optimization of Distributed Energy Resources (DER)

    2. b. Consumption optimization of energy bought on wholesale market

3. Participation into balancing and ancillary services

4. Microgrid-as-a-Service

In the FLEXCoop business scenarios, as in many other projects and applications, the ESS has typically two main missions:

- **Maximize self-consumption**, of locally produced renewable energy (business model 2.a). In this situation the ESS stores excess of renewable energy production (generation peaks) to be used in other moments. As described in the FLEXCoop business scenario: *"The REScoop uses consumer flexibility to better match the patterns of the coop's generation assets – owned by prosumers or owned by the cooperative as generator (VPP as a REScoop resource)"*
- **Reduce customer electric energy bill** optimising its energy consumption patterns (business model 2.b). In this situation the ESS stores electric energy to be used in periods of high energy prices. As described in the FLEXCoop business scenario: *"The cooperatives use consumer flexibility to better match the anticipated prices on wholesale market – encouraging consumption at low hours and avoiding consumption at peak hours (use of dynamic prices, the cooperative may propose a cheaper tariff in exchange of accessing consumers flexibility)"*

Main benefits of both business models are better integration of RES and reduced energy bills. In the first case, integration of RES production is the main objective of optimisation, but in the end, this is done in order to maximise use of local resources and thus, reduce bills for imported energy. In the second case, reduction of energy bills is the main objective, without the need of having RES installed. Nevertheless, dynamic price signals are heavily influenced by RES generation in the grid. If the market mechanisms are working well, high RES generation will lead to lower electricity prices. Price fluctuations are larger, if system flexibility is lower. Therefore, if flexibility is introduced into the system, RES integration is improved [17].

FLEXCoop business scenarios are based on consumer flexibility, understood as the consumer ability to modify its consumption patterns to external signals: renewable production in 2.a and electric energy prices in 2.b. An important obstacle to use this flexibility is the reluctance of customers to adapt their habits to external signals. Some authors state that a solution could be to combine automatic control systems with a local ESS which can modulate demand patterns without any inconvenience for the customer [18].

Customer flexibility can also be used to provide balancing and ancillary services as proposed in business scenario 3. These services can be amplified using ESS. In fact, one of the primary sources of revenue for many energy storage projects built to date is providing ancillary service [19].

The last FLEXCoop business scenario (4) also has an important dependence on ESS. To become independent of the electric grid using renewable energy sources it is mandatory to use storage systems, in order to balance energy generation and consumption.

ESS can be placed in customer facilities as standalone or grid-connected solution [18]. Currently, there are many producers and dealers of storage systems that commercialize systems that are becoming more secure, efficient and cheaper [19]. Some of these manufacturers (for example: KOKAM [20], ENPHASE [21], VARTA [22], TESLA [23], ENERSYS [24]) have specific products adapted for residential customers that can improve the flexibility of the electric consumers. Although the last example still relies on lead-acid batteries, many manufacturers offer solutions based on lithium ion technology. Market products have different values of power and energy capacity, adapted to residential customers with different consumption characteristics, starting from a 1.6 kW/3.6 kWh system. The main variables that determine the characteristics and use of an ESS are:

- Rated energy capacity (E_{ESS}) – Amount of energy [kWh] that can be stored in the ESS.
- Charging and discharging efficiency (η_{charge} and $\eta_{discharge}$) – Percentage [%] of the energy stored and taken back from the batteries from the total.
- Max. discharging power ($P_{discharge\_max}$) – Maximum power [kW] that can be supplied by the storage system.
- Max. charging power (P_{charge_max}) – Maximum power [kW] that can be supplied to the storage system.
- Minimum state of charge (SoC_{min}) – Percentage [%] of capacity or capacity [kWh] of the batteries under which the storage must not be used, in order to conserve its integrity and nominal parameters.
- Maximum state of charge (SoC_{max}) – Percentage [%] of capacity or capacity [kWh] of the batteries over which the storage should not be used, in order to conserve its integrity and nominal parameters.
- Lifetime (n_{cyc}) – Time duration for which the storage keeps its parameters. This value can be measured in time [years] or charging-discharging cycles [cycles].
- Initial costs (C_{Inv}) – Costs of purchasing and installing the ESS, which typically have a power related [€/kW] and an energy related [€/kWh] component.
- O&M costs ($C_{O\&M}$) – Operation and maintenance costs related to the use of the ESS [€/cycle or €/kWh].
- Charging and discharging efficiency of the power converter (η_{pc_charge} and $\eta_{pc\_discharge}$) – Percentage [%] of the energy taken from the batteries and sent to the grid and vice versa.
- Maximum charging and discharging power of the power converter ($P_{pc\_charge\_max}$ and $P_{pc\_discharge\_max}$). Maximum and minimum active power [kW] of the power converter. If the converter can regulate the reactive power (Q(t)) it is expressed in terms of apparent power $S_{pc\_charge\_max}$ and $S_{pc\_discharge\_max}$ [kVA].

These variables and the State of Charge (SoC, amount of energy stored in the storage system as a part of the rated energy capacity and usually measured in kWh or as a percentage [%] of

the rated energy capacity of the batteries) are essential to describe the characteristics of the ESS in a model. There are many ESS modelling methodologies depending on the phenomena to be analysed or usage, as for example: ageing of the batteries, effect on power quality, sizing of a storage system, real-time operation.

The modelling shown in the next two sections is developed to control/operate the ESS in real-time. For this reason, these models will use physical/electrical variables (as rated energy capacity, efficiency or SoC for example) and economical/operative variables (as lifetime or initial and O&M costs).

In the following sections, stationary ESS and Vehicle-as-ESS are distinguished. First, the stationary system is described, and then, additional model variables are introduced, in order to take into account peculiarities of the electric vehicle.

5.1. DER Modelling

5.1.1. Batteries, stationary systems

For simplicity and because this is the most common application, the stationary ESS is described here as a battery energy system (BES), but the basic model can be applied also to a fuel cell or a redox flow battery.

Apart from the battery, an ESS contains also other subsystems, as shown in Figure 11: battery management system (BMS), AC/DC power converter, electric protections and auxiliary systems, such as cooling or gas extractors if needed. All of these systems have to be included in the economic variables but only the power converter characteristics have to be included in the economic/operative variables. The importance of the converter in the model is due to its function: adapting AC current of the grid to DC current to be feed to the batteries and vice versa.

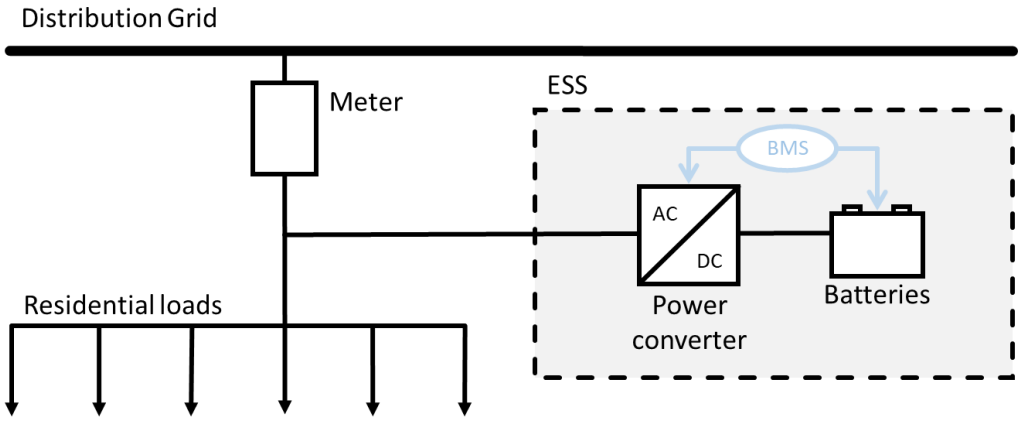

Figure 11: Example of an ESS of a residential customer

The proposed model has been developed to be used in optimization processes whose results are the operation set-points for an ESS. Figure 12 shows the power flows involved in the ESS model described below.

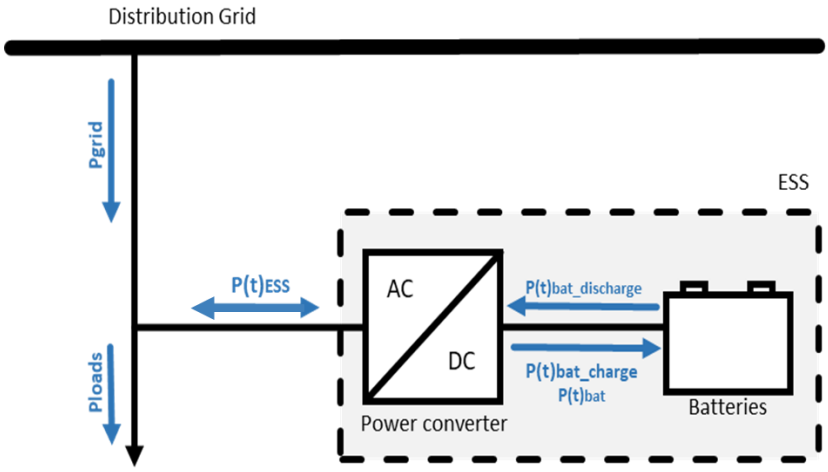

Figure 12: Power flows in the model of an ESS

$$SoC_{min} \leq SoC(t) \leq SoC_{max} \quad (15)$$

The state of charge of the ESS batteries (SoC(t)) must be, along all the optimization period, equal or lower than the maximum state of charge (SoC_{max}) and equal o higher than the minimum state of charge (SoC_{min}). In most of the systems, $SoC_{max}=E_{ESS}$.

$$SoC(t) = SoC(t-1) + \left[P(t)_{bat\_charge} \cdot \eta_{charge} - P(t)_{bat\_discharge}/\eta_{discharge}\right]\Delta t \quad (16)$$

The current state of charge of the ESS batteries, SoC(t), is equal to the previous one, SoC(t-1), plus the energy charged in the batteries and minus the energy discharged including the efficiency of the batteries.

$$0 \leq P(t)_{bat\_charge} \leq availability(t) * P_{charge\_max} \quad (17)$$

$$0 \leq P(t)_{bat\_discharge} \leq availability(t) * P_{discharge\_max} \quad (18)$$

When available, batteries charging and discharging power must be lower or equal to the maximum. availability(t) is 0 when the ESS is not available and 1 when it is available.

$$P(t)_{bat} = P(t)_{bat\_charge} - P(t)_{bat\_discharge} \quad (19)$$

$$P(t)_{ESS} = P(t)_{bat} + P(t)_{pc\_losses} \quad (20)$$

$$-P_{pc\_discharge\_max} \leq P(t)_{ESS} \leq P_{pc\_charge\_max} \quad (21)$$

ESS power must be between the limits of the power converter ($P_{pc\_charge\_max}$ and $P_{pc\_discharge\_max}$) and the power that enters the ESS is equal to the addition of the battery power and the power converter losses.

If the power converter can regulate reactive power, for example to compensate the reactive power demand of the domestic loads, another equation has to be added to the model.

$$P(t)_{ESS}{}^2 + Q(t)_{ESS}{}^2 \leq S_{\text{pc\_charge\_max}}{}^2 \quad (22)$$

$$C_{ESS} = \frac{C_{INV}+C_{O\&M}}{2\, n_{\text{cyc}}\, E_{ESS}} \left(P(t)_{bat\_charge} + P(t)_{bat\_discharge}\right) \Delta t \quad (23)$$

Finally, the cost of using the ESS has to be modelled. Equation (23) shows the cost of using the ESS, derived from the wear each cycle charging/discharging produces to the ESS.

To apply this model to a business scenario such as 2.b, besides the forecast of energy consumption in the residential loads and energy prices, only the ESS availability forecast, availability(t), is needed. For example, a maintenance process that disables the system should be reflected by this ESS availability forecast.

5.1.2. EVs as ESS (V2G)

Passenger cars are parked most of the time. In fact, some data show that cars are parked 90-95% of the time, either at home, street lots, commercial areas or at work [27]. This fact, in addition to the increasing amount of electric vehicles (EV), has made that many researchers and institutions propose the Vehicle-to-Grid (V2G) capability of electric vehicles (EV acting as stationary batteries) as the next stage in the development of EV and its integration in the smart grids of the future [28].

V2G [29] basically means, that EV batteries are used in a very similar manner, as stationary batteries. Therefore, it provides the same services such as: integration of renewable generation, grid services such as voltage and frequency control, supply emergency backup power, peak shaving and valley filling, to give some examples [28], [30], [31]. Therefore, EV batteries can be used as stationary ESS. In the following paragraphs, the differences of the V2G model comparted to the stationary ESS are described.

Besides its functionalities as ESS, specific characteristics of its use as EV must be included in the model:

- EV availability at the charging point ($V2G\_availability(\text{t})$). $V2G\_availability(\text{t})$ is 0 when the EV is not available as an ESS and 1 when it is available.
- Minimum SoC at departures and minimum SoC when connected to the charging point.
- EV consumption when operating as a vehicle ($P_{EV}(t)$).

Stationary ESS are available most of the time, only failures or maintenance tasks can put them out of service. In contrast, the availability of an electric vehicle at a charging point depends on the usage pattern of its drivers. Consequently, more effort has to be invested in the availability forecast of the EV as a storage system.

The main purpose of an EV is transportation (people and objects) and not its use as ESS. Therefore, its usage and availability is subject to its use as a means of transport. For example, at expected departures, the EV batteries should have a pre-established SoC related to the trip to be carried out not to its use as ESS. Another example is that when connected to the charging point, the minimum SoC could be related to possible emergency trips and not to the minimum

advisable state of charge of the EV batteries. Consequently, the minimum SoC of an EV used as ESS is not the minimum SoC of the batteries, it is derived from its use as a vehicle and may vary along time.

As seen in section 5.1.1, for an ESS there are only two power flows: charging and discharging batteries. In an EV, batteries have a third power flow: the energy supplied to the vehicle engines, while it is disconnected from the charging point. This characteristic has to be included in the model and in the needed forecasts.

According to these specific characteristics, only small changes have to be done starting from the ESS model: the minimum SoC of the batteries varies with time in Equation (15) and the EV consumption when driving in Equation (16).

$$SoC_{min}(t) \leq SoC(t) \leq SoC_{max} \tag{24}$$

$$\begin{aligned} SoC(t) = SoC(t-1) \\ + \left[P_{bat\_charge}(t) \cdot \eta_{charge} - \frac{P_{bat\_discharge}(t)}{\eta_{discharge}} \right. \\ \left. - \left(1 - V2G\_availability(\mathrm{t})\right) P_{EV}(t) \right] \Delta t \end{aligned} \tag{25}$$

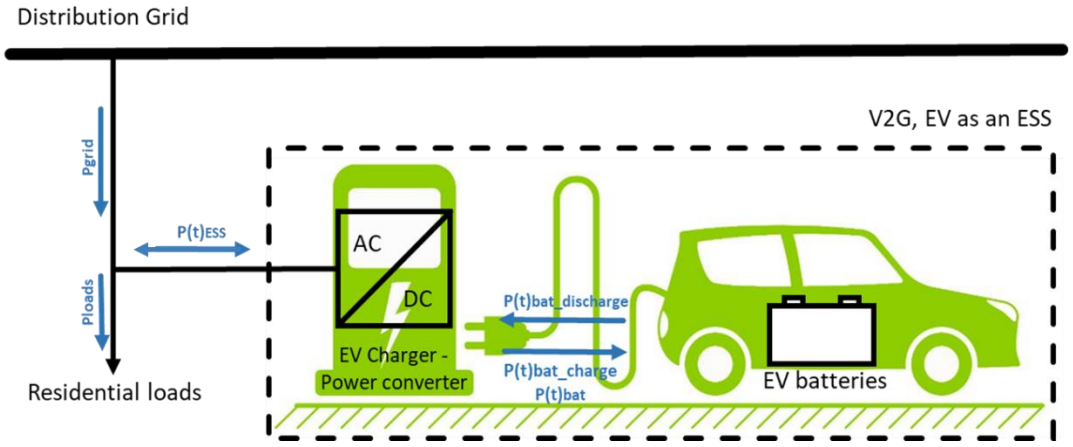

Figure 13: Power flows in the model of an EV acting as an ESS

To apply such a model, besides the forecast of energy consumption of the residential loads and energy prices, other forecasts are needed:

- EV availability at the charging point.
- EV SoC at arrival to the charging point and EV power consumption (P_{EV}) when operating as a vehicle.
- EV minimum SoC when the EV is at the charging point.
- Individual driving patterns, etc.

However, all these parameters will be considered and examined in detail in the T3.4 regarding the provision of accurate and robust profiling of EV flexibility (definition of individual EVs

profiles). Thus, they will not be further analysed here because it is out of the scope of this deliverable.

5.1.3. DER model parameters

The table below summarises the storage model parameters (input/output) in previous sections.

Table 3: Storage systems DER Model Parameters (defined per storage unit)

PARAMETER	DESCRIPTION	UNITS	TYPE
Input Parameters			
E_{ESS}	Rated energy capacity	kWh (or Wh)	Float
η_{charge} and $\eta_{discharge}$	Charging and discharging efficiency	%	Float
P_{charge_max} and $P_{discharge\_max}$	Maximum charging and discharging power	kW (or W)	Float
SoC_{max} and SoC_{min}	Maximum and minimum state of charge	%	Float
n_{cyc}	Lifetime	Years of cycles	Float
C_{Inv} and $C_{O\&M}$	Initial and Operations and Management (O&M) costs	€/kW and €/cycle or €/kWh	Float
η_{pc_charge} and $\eta_{pc\_discharge}$	Charging and discharging efficiency of the power converter	%	Float
$P_{pc\_charge\_max}$ and $P_{pc\_discharge\_max}$ (or $S_{pc\_charge\_max}$ and $S_{pc\_discharge\_max}$)	Maximum charging and discharging power of the power converter	kW (or W) (kVAr or VAr)	Float
Previous SoC	SoC of the ESS, previous to the optimization step	%	Float
Availability	Availably of the ESS to be used	1/0	Boolean
P_{EV}	EV power consumption when driving	kW (or W)	Float
Output Parameters			
SoC	Objective SoC of the batteries	% (or Wh)	Float
$P(t)_{ESS}$ and $Q(t)_{ESS}$	Charge/discharge power and reactive power of the ESS	W and VAr	Float

6 Generation forecasting

The aim of this section is to present a way to setup statistical models, which can be used for generation forecasting, e.g. wind and solar power. They can be fitted using weather forecasts as input – thus providing a setup for online forecasting. The general challenge is that weather forecasts are used, which leads to "overlapping" time series. For example, in many settings where hourly forecasts are needed, with a horizon up to 48 hours ahead, they must be updated every hour with the latest weather forecasts as input. This gives rise to two challenges: First the weather forecasts are not updated every hour, so we need ways to use the most recent weather forecasts, and second we need to set this up in order to fit the models in a way, which is both easy to use and effective, both in terms of forecast performance and computational resources. It is further noted, that the models can easily be setup using the latest observations as input, thus making them suitable for both very-short term (<6 hours) and short-term (2-3 days) forecasts. The technique is first presented in a generic way and in the last part of this section examples applying it for solar forecasting are presented.

6.1 Forecasting literature review

Time series modelling is one of the major tools which has been used quite extensively both by engineering and scientific communities over last few decades to model the dynamic phenomenon or systems. The main aim of the time series modelling is to develop or apply rigorous statistical methods to capture the dynamical information present in the measured data. Time series models study the past observations of a predictor variables (also known as the feature variables of the time series) to develop an appropriate model which can describe the inherent structure of the time series as well as predict the response variable. This developed model is then finally used to make short or long term forecasts. Time series forecasting thus can be termed as the act of predicting the future by understanding the past [32, 33]. Time series forecasting is of indispensable importance to numerous practical fields such as business, economics, finance, science and engineering, etc. [34, 35] . Therefore, one must take proper care to identify a model with proper structure adequate to describe the dynamics of the underlying time series. Furthermore, an appropriate model estimation and validation criteria is of utmost importance for time series forecasting. A lot of efforts have been put by researchers over many years for the development of efficient model estimation algorithms to improve the forecasting accuracy. As a result, a plethora of methods for time series forecasting models have been reported in the literature.

6.1.1 Solar forecasting

Many approaches to solar power forecasting have been suggested during more than a decade. Some of the first literature is from [36] who make sub-hourly forecasts by normalizing with a clear sky model and using arima models. [37] use neural networks to make one-step predictions of hourly values of global irradiance and compare these with linear time series models that work by predicting clearness indexes. [38] use satellite images for horizons below 6 hours, and in

[39] numerical weather predictions (NWPs) for longer horizons, as input to neural networks to predict global irradiance. This is transformed into solar power by a simulation model of the PV system. [40] investigate feed-forward neural networks for one-step predictions of hourly values of global irradiance and compare these with seasonal auto-regressive models applied on solar power directly. [41] use neural networks combined with wavelets to predict next day hourly values of global irradiance. Different types of meteorological observations are used as input to the models; among others the daily mean global irradiance and daily mean cloud cover of the day to be forecasted. [42] use weather forecasts to predict hourly solar intensity as a proxy for solar power generation. The study compares multiple regression techniques for generating prediction models, including linear least squares and support vector machines using multiple kernel functions. Furthermore, dimensionality reduction is explored using principal component analysis. Similarly, [43] propose a model based on support vector machines for forecasting of PV power, where multiple techniques for dimensionality reduction of the input variables are exploited. These results clearly support the importance of proper feature and model selection. The paper takes advantage of the automated feature selection of the gradient boosted regression trees. [44] propose the use of Artificial Neural Networks to forecast global radiation and direct radiation using weather forecasts as predictors. A preliminary feature selection is performed using a genetic algorithm and a gamma test. [45] fit several forecasting models, which predict the hourly PV power generation for one and two hours ahead only using endogenous variables. The methods studied in the paper are among others arima, k-nearest-neighbors and neural networks optimized by genetic algorithms. Tree based models have also been applied for probabilistic forecasting of solar power generation, e.g. [46] and [47] successfully apply quantile regression forests to estimate quantiles of the PV power generation in order to produce probabilistic forecasts.

6.1.2 Background of presented generation forecasting models

The forecasting approach described in this section are inspired by a setup used for forecasting of heat load in district heating, as described in [48] and [49]. It is applied in different settings for load forecasting by [50], [51], [52] and [53]. The approach has been further developed to encompass the possibility to model many kind of functional relationships, both dynamics and non-linear. Thus now provides a sound framework for online forecasting of generation in many settings. More specifically, the setup can also be used to fit the models suggested by [50] and extends even further, potentially also encompassing wind power forecast models presented by [54] and [55].

6.1.3 Statistical model notation

The notation in this section is following [56] as far as possible.

Generally, in statistical notation uppercase Latin letters are used to denote random variables, e.g. the simplest linear would model

$$Y_t = \beta_0 + \beta_1 u_t + \varepsilon_t \tag{26}$$

where

- the output Y_t is a random variable
- the input u_t is an input
- the error is a random variable $\varepsilon_t \sim N(0, \sigma^2)$ and independent and identically distributed (i.i.d.) (thus also Greek letters are denoting random variables, however for them upper- and lowercase are not distinguished)
- the parameters β_0 and β_1 are actually also random variables

The actual observations are denoted with small letters

$$y_t \tag{27}$$

and the predictions are

$$\hat{y}_t = \hat{\beta}_0 + \hat{\beta}_1 u_t \tag{28}$$

where the hat ˆ indicates an estimated or predicted value.

Further, the realization of the error (ε_t) is the residual

$$\hat{\varepsilon}_t = e_t = y_t - \hat{y}_t \tag{29}$$

hence either denoted with a hat or with a lowercase Latin letter.

However, this is not always possible to keep this notation, firstly in physics uppercase Latin letters are used, e.g.

- G_t is the global radiation ($\mathrm{W\,m^{-2}}$)

Matrices and vectors are marked with bold.

6.1.4 Indexing using t and k

In the present document all time series considered are equidistant sampled and the sampling period is normalized to 1, hence the time t is simply an integer, which index the value of a variable at t. The same goes for horizon k, which index a prediction k steps ahead in time.

Further, in the generic setup a forecast at each time t is calculated for each horizon k up to n_k ahead. To achieve a notation which can deal with overlapping time series, a two dimensional index is needed. The most widespread notation is

$$u_{t+k|t} \tag{30}$$

which means: the value of variable x, at time $t+k$, and *conditional* the information available at time t. The bar conditional is indicated by the bar $|$.

Thus for $k > 0$ this is a forecast, usually an NWP of the input, however it can also be deterministic input, e.g. a Fourier series, which is known ahead in time (in this case the conditional notation ($|$) should not be kept).

For $k \leq 0$ some ambiguity is also possible, since observations can be used

$$u_{t+k|t} = u^{\text{obs}}_{t+k} \text{ for } k \leq 0 \tag{31}$$

however the NWP can also be used

$$u_{t+k|t} = u^{\text{nwp}}_{t+k|t} \text{ for } k \leq 0 \tag{32}$$

thus a value for the past time can come from an NWP, which was not available before time t.

These aspects will be more clear in later sections as it is explained how data is setup and updated in online settings.

6.2 Forecast model input and output

Input, for which we have a forecast, e.g. NWP inputs, we set up, at time t, an input matrix for the variable with name **nm**. It holds for each time t *the latest available forecasts along the row*

$$\boldsymbol{u}^{\text{nm}}_t = \begin{array}{c} \begin{array}{ccccccc} \textbf{k0} & & \textbf{k1} & \textbf{k2} & \dots & \textbf{kxx} & \textbf{horizon/time} \end{array} \\ \begin{pmatrix} u^{\text{nm}}_{t_0|t_0} & u^{\text{nm}}_{t_0+1|t_0} & u^{\text{nm}}_{t_0+2|t_0} & \dots & u^{\text{nm}}_{t_0+n_k|t_0} & t_0 \\ u^{\text{nm}}_{t_1|t_1} & u^{\text{nm}}_{t_1+1|t_1} & u^{\text{nm}}_{t_1+2|t_1} & \dots & u^{\text{nm}}_{t_1+n_k|t_1} & t_1 \\ \vdots & \vdots & \vdots & & \vdots & \vdots \\ u^{\text{nm}}_{t-1|t-1} & u^{\text{nm}}_{t|t-1} & u^{\text{nm}}_{t+1|t-1} & \dots & u^{\text{nm}}_{t-1+n_k|t-1} & t-1 \\ u^{\text{nm}}_{t|t} & u^{\text{nm}}_{t+1|t} & u^{\text{nm}}_{t+2|t} & \dots & u^{\text{nm}}_{t+n_k|t} & t \end{pmatrix} \end{array} \tag{33}$$

where

- t is the counter of time for equidistant time points and the sampling period is 1 (note that it is not included in the matrix, it is simply the row number)
- t_0 is the first available time point
- n_k is the length of the forecasting horizon

- The column names are indicated above the matrix, they are simply a **k** concatenated with the value of k.

Hence, with a prediction horizon $n_k = 24$, having data from time $t = 1$, then at time $t = 100$ we would have the following matrix

$$\boldsymbol{u}_t^{\mathrm{nm}} = \begin{array}{c} \begin{array}{ccccc} \textbf{k0} & \textbf{k1} & \textbf{k2} & \dots & \textbf{k24} \end{array} \\ \begin{pmatrix} u_{1|1}^{\mathrm{nm}} & u_{2|1}^{\mathrm{nm}} & u_{3|1}^{\mathrm{nm}} & \dots & u_{25|1}^{\mathrm{nm}} \\ u_{2|2}^{\mathrm{nm}} & u_{3|2}^{\mathrm{nm}} & u_{4|2}^{\mathrm{nm}} & \dots & u_{26|2}^{\mathrm{nm}} \\ \vdots & \vdots & \vdots & & \vdots \\ u_{99|99}^{\mathrm{nm}} & u_{100|99}^{\mathrm{nm}} & u_{101|99}^{\mathrm{nm}} & \dots & u_{123|99}^{\mathrm{nm}} \\ u_{100|100}^{\mathrm{nm}} & u_{101|100}^{\mathrm{nm}} & u_{102|100}^{\mathrm{nm}} & \dots & u_{124|100}^{\mathrm{nm}} \end{pmatrix} \end{array} \begin{array}{c} \textbf{horizon/time} \\ 1 \\ 2 \\ \vdots \\ 99 \\ 100 \end{array} \tag{34}$$

This could for example be the forecasts of the global radiation

$$\boldsymbol{G}_t = \begin{array}{c} \begin{array}{ccccc} \textbf{k0} & \textbf{k1} & \textbf{k2} & \dots & \textbf{kxx} \end{array} \\ \begin{pmatrix} G_{t_0|t_0} & G_{t_0+1|t_0} & G_{t_0+2|t_0} & \dots & G_{t_0+n_k|t_0} \\ G_{t_1|t_1} & G_{t_1+1|t_1} & G_{t_1+2|t_1} & \dots & G_{t_1+n_k|t_1} \\ \vdots & \vdots & \vdots & & \vdots \\ G_{t-1|t-1} & G_{t|t-1} & G_{t+1|t-1} & \dots & G_{t-1+n_k|t-1} \\ G_{t|t} & G_{t+1|t} & G_{t+2|t} & \dots & G_{t+n_k|t} \end{pmatrix} \end{array} \begin{array}{c} \textbf{horizon/time} \\ t_0 \\ t_1 \\ \vdots \\ t-1 \\ t \end{array} \tag{35}$$

All values where $k \geq 1$ naturally have to be forecasts of the inputs, e.g. for the global radiation these will come from an NWP. If there are local observations available of the input the past

values can be taken from the observations

$$\boldsymbol{G}_t = \begin{array}{c} \begin{array}{ccccccc} \textbf{k0} & & \textbf{k1} & \textbf{k2} & \dots & \textbf{kxx} & \textbf{horizon/time} \end{array} \\ \begin{pmatrix} G^{\text{obs}}_{t_0|t_0} & G^{\text{nwp}}_{t_0+1|t_0} & G^{\text{nwp}}_{t_0+2|t_0} & \dots & G^{\text{nwp}}_{t_0+n_k|t_0} & t_0 \\ G^{\text{obs}}_{t_1|t_1} & G^{\text{nwp}}_{t_1+1|t_1} & G^{\text{nwp}}_{t_1+2|t_1} & \dots & G^{\text{nwp}}_{t_1+n_k|t_1} & t_1 \\ \vdots & \vdots & \vdots & & \vdots & \vdots \\ G^{\text{obs}}_{t-1|t-1} & G^{\text{nwp}}_{t|t-1} & G^{\text{nwp}}_{t+1|t-1} & \dots & G^{\text{nwp}}_{t-1+n_k|t-1} & t-1 \\ G^{\text{obs}}_{t|t} & G^{\text{nwp}}_{t+1|t} & G^{\text{nwp}}_{t+2|t} & \dots & G^{\text{nwp}}_{t+n_k|t} & t \end{pmatrix} \end{array} \tag{36}$$

Note, that in most cases there is a bias between the NWPs and local observations, thus a model must be applied in a step before fitting the forecast models – such aspects are not dealt with in this report.

6.2.1 Updating an NWP input matrix

One can choose either to update the input matrix in each time step or when a new NWP is received.

6.3 Two-stage modelling procedure

In order to model non-linear functional relations between inputs and output a two-stage modelling procedure is used. This is a widespread approach, see [57], since it allows to fit complex models with robust and fast estimation techniques. First, in the *transformation stage*, some function of the inputs, e.g. low-pass filtering, spline or Fourier basis, etc., can be applied (cf. f_1 and f_2 below in Equation (37)). Second, in the *regression stage*, a regression model is applied to fit a function between the transformed inputs and the output – the parameters are fitted for each horizon.

Lets go through it with a simple example, first the transformation stage

$$\begin{aligned} \text{Intercept:} \quad & \mu_{t+k|t} = 1 \\ \text{Regressor 1:} \quad & x^{\text{nm1}}_{t+k|t} = f_1(\boldsymbol{u}^{\text{nm1}}_t; \boldsymbol{\theta}_{\text{nm1}}) \\ \text{Regressor 2:} \quad & x^{\text{nm2}}_{t+k|t} = f_2(\boldsymbol{u}^{\text{nm2}}_t; \boldsymbol{\theta}_{\text{nm1}}) \end{aligned} \tag{37}$$

and then the regression stage

$$Y_{t+k|t} = \beta_{0,k}\mu_{t+k|t} + \beta_{1,k}x^{\text{nm1}}_{t+k|t} + \beta_{2,k}x^{\text{nm2}}_{t+k|t} + \varepsilon_{t+k|t} \tag{38}$$

Thus, this model has:

- Intercept: $\mu_{t+k|t}$
- Two inputs (matrices): $\boldsymbol{u}^{\text{nm1}}_{t+k|t}$ and $\boldsymbol{u}^{\text{nm1}}_{t+k|t}$
- Output: $Y_{t+k|t}$
- Transformation parameters (vectors): $\boldsymbol{\theta}_{\text{nm1}}$ and $\boldsymbol{\theta}_{\text{nm2}}$
- Regression parameters for each horizon k: $\beta_{0,k}$, $\beta_{1,k}$ and $\beta_{2,k}$

The regression parameters are estimated with a closed form scheme, most simple is a linear least squares regression, however this can be extended to a recursive or local version, more on this later. The transformation parameters must be estimated with some heuristic optimization.

6.3.1 Transformations stage

In the first stage the inputs are transformed with some function, mostly either a recursive function (filtering to model a dynamical system) or some basis function (splines or Fourier series applied to model non-linear functions).

Filtering

When modelling the output of a (linear) dynamical system a "trick" is to apply a filter directly on the input (instead of applying an armax model [56]).

The input time series is filtered with a transfer function

$$x_t = H(B;a)u_t \tag{39}$$

where B is the backshift operator (see [33]) and a is a parameter. The simplest 1st order low-pass with gain of 1 is

$$H(B;a) = \frac{1-a}{1-aB} \tag{40}$$

thus

$$H(B;a)u_t = \frac{(1-a)u_t}{1-au_{t-1}} \tag{41}$$

thus we have a filter coefficient a between 0 and 1, which must be tuned to match the particular time constant of the linear system.

Now, this is stated slightly simpler than in Equation (37), where a full input matrix is input to the transformation function. In particular, such a filter can be applied in two ways, either along the columns in $\boldsymbol{u}_t$, see the its definition in Equation (33, such that

$$x_{t+k|t} = \frac{(1-a)u_{t+k|t}}{1-au_{t-1+k|t-1}} \tag{42}$$

or along the rows

$$x_{t+k|t} = \frac{(1-a)u_{t+k|t}}{1-au_{t+k-1|t}} \tag{43}$$

To illustrate the effect of low-pass filtering the plot the plot in Figure 14 shows the response to a step function for different filter coefficients a. It is clearly seen that the responses are exponen-

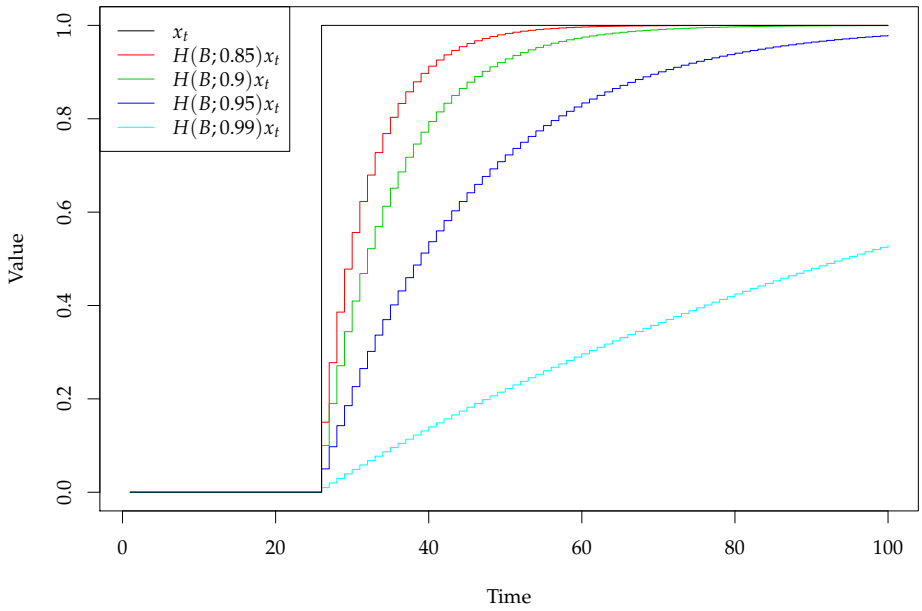

Figure 14: The response to a step function for different filter coefficients a.

tial functions with different time constants depending on the value of a, such that a higher value results in a slower response. This filter is equivalent to a single resistor and capacitor system, hence a first order auto-regressive (i.e. arx) model, with a stationary gain of 1. If needed higher order filter can be selected for the pre-treatment of the data but a proper care must be taken. Higher order filter may suppress some part of the dynamical information present in the data.

Base splines

A wide spread approach to model non-linear functional relations is to apply spline basis functions [57]. The basic idea is to "resolve" a single input time series into several time series, which levels depends on the input time series. Thereafter a linear combination of the time series (fitted in the regression stage) results in a non-linear spline function of the input time series.

Thus, the spline basis function

$$\boldsymbol{x}_t = f_{\text{bspline}}(u_t; n_{\text{deg}}) \tag{44}$$

where n_{deg} is the degree of the piecewise polynomial function, hence a higher n_{deg} results in a more "flexible" function. Note that $\boldsymbol{x}_t$ is a vector, since the transformation results in n_{deg} variable. The places where the piecewise polynomial meet are known as knots. The key property of spline functions is that they and their derivatives may be continuous, depending on the multiplicities of the knots. The input is resolved with spline basis functions, e.g. for an input in the interval $[0,1]$ the basis splines for $n_{\text{deg}} = 4$, as plotted in Figure 15. The vertical dashed horizontal lines marks the knot points (must be set in some way, usually set as equidistant quantiles of values of u_t).

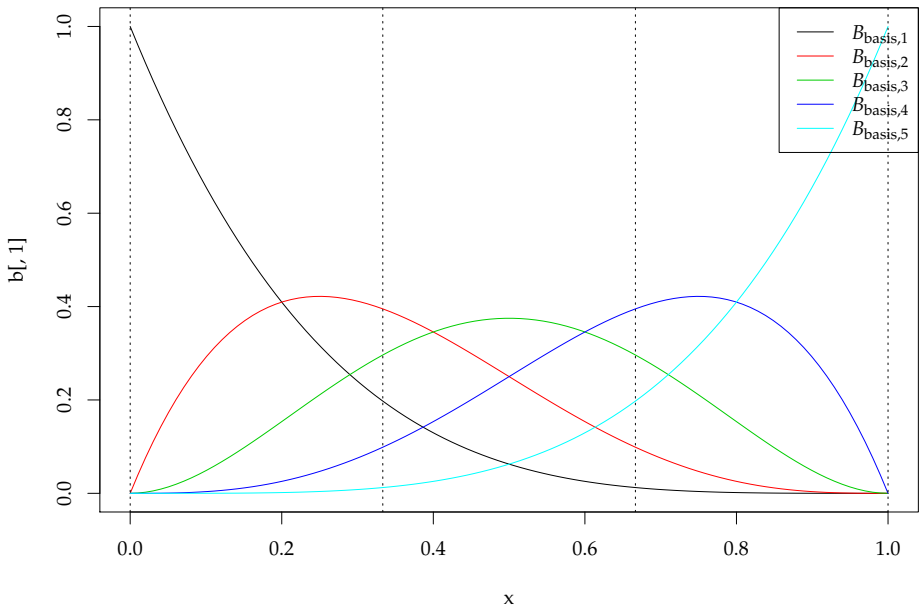

Figure 15: The basis splines for $n_{\text{deg}} = 4$ with an input in the interval $[0,1]$. The vertical dashed horizontal lines marks the knot points.

An example is presented, where a non-linear function with some added noise is simulated (simply numbers generated with the computer). Using the generated observations the function can be estimated using the basis functions. First a non-linear function with some added noise is simulated

$$Y_i = \begin{cases} u_i^3 + \varepsilon_i \text{ for } u_i \leq 0 \\ u_i^3 - 0.5 + \varepsilon_i \text{ for } u_i > 0 \end{cases} \tag{45}$$

where $\varepsilon \sim N(0, 0.1^2)$ and independent and identically distributed (i.i.d.). A sample of 100 observations is simulated and spline basis functions of increasing degree is generated and used as input to a linear regression model. The resulting spline functions modeled is seen in the plot in Figure 16. It is clear that there is a balance between bias and variance: A too low degree results in an under-fitted model (not able to "bend" enough), while a too high degree results in an over-fitted model (bends to much). The degrees of freedom can be optimized using a cross-validation approach.

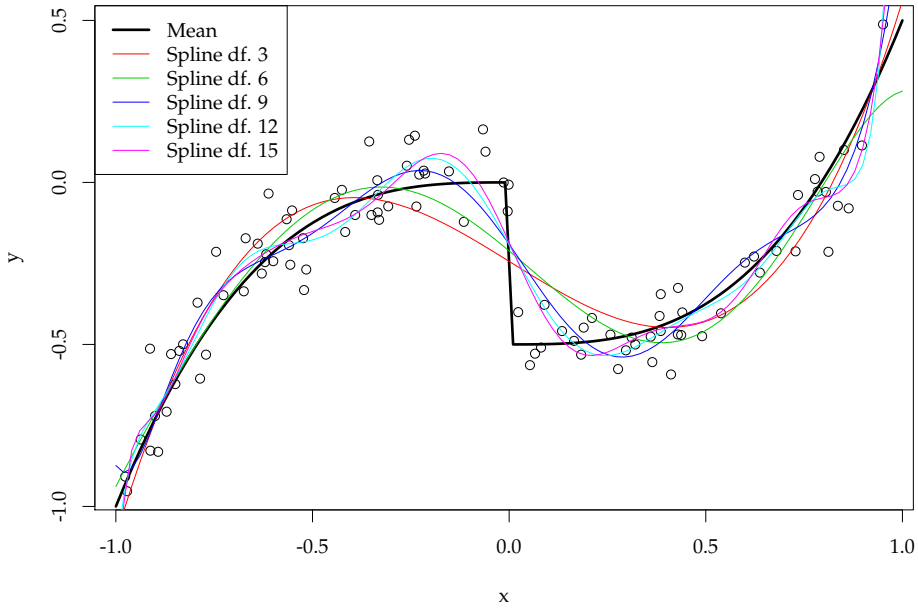

Figure 16: Resulting spline functions from the model example in Equation (45).

Fourier series

In order to model periodic phenomena a linear combination of Fourier series is a very effective approach.

We use the notation

$$\boldsymbol{x}_t = f_{\text{fs}}(u_t; n_{\text{har}}) \tag{46}$$

where n_{har} is the number of harmonic pairs included, hence $\boldsymbol{x}_t$ is vector of length $2n_{\text{har}}$, which is then linearly combined in the regression stage. Exemplified with time as input $u_t = t$ (which is often done when modelling period, e.g. diurnal or yearly phenomena)

$$\left[\sin\left(\frac{2\pi}{t_{\text{per}}}t\right) \quad \cos\left(\frac{2\pi}{t_{\text{per}}}t\right) \quad \sin\left(\frac{2\cdot 2\pi}{t_{\text{per}}}t\right) \quad \cos\left(\frac{2\cdot 2\pi}{t_{\text{per}}}t\right)\right. \tag{47}$$

$$\ldots \tag{48}$$

$$\left.\sin\left(\frac{n_{\text{har}}2\pi}{t_{\text{per}}}t\right) \quad \cos\left(\frac{n_{\text{har}}2\pi}{t_{\text{per}}}t\right)\right] \tag{49}$$

An example of Fourier basis functions is plotted below in Figure 17 for $n_{\text{har}} = 3$, hence 3 pairs of harmonics and a period $t_{\text{per}} = 1$.

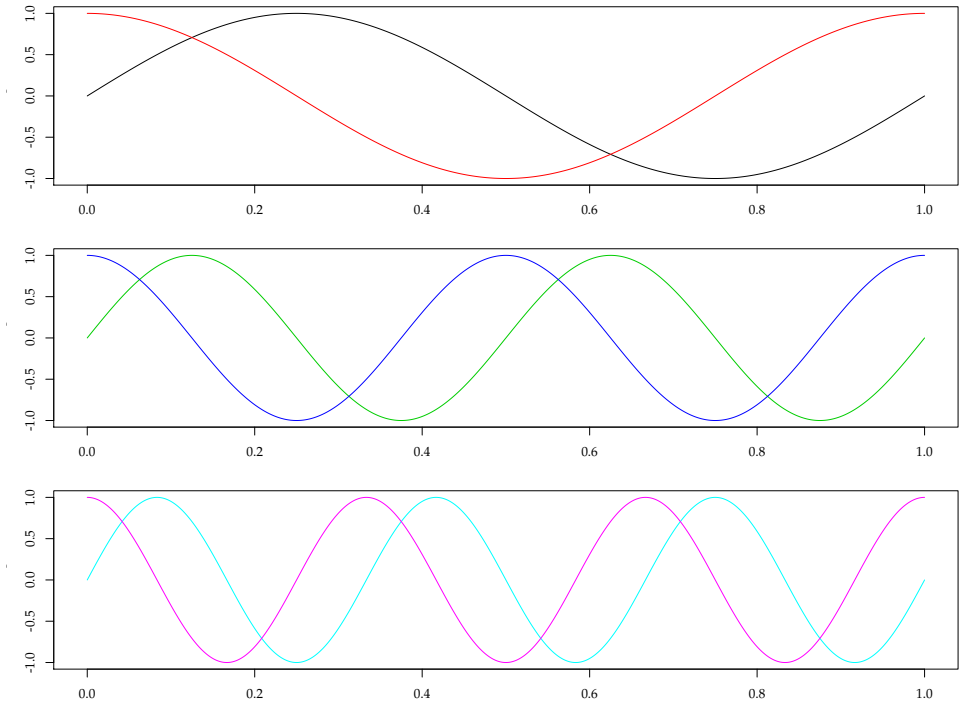

Figure 17: Fourier basis functions for $n_{\text{har}} = 3$.

Combined transformations

It is perfectly possible to combine transformations to create models involving complicated functions. E.g. first a low-pass filter and then a spline basis

$$\boldsymbol{x}_t = f_{\text{bspline}}(H(B;a)u_t; n_{\text{deg}}) \tag{50}$$

or basis splines and which are then low-pass filtered

$$\boldsymbol{x}_t = f_{\text{bspline}}(u_t; n_{\text{deg}}) \tag{51}$$

Thus in both cases the result is multiple variables ($\boldsymbol{x}_t$ is a vector) and transformation parameters are $\boldsymbol{\theta} = [a, n_{\text{deg}}]$.

6.3.2 Regression stage

In the regression stage the coefficients are estimated for each horizon k. For a linear least squares regression, this is written by

$$Y_{t+k|t} = \beta_{0,k} + \beta_{1,k} x_{t+k|t} + \varepsilon_{t+k|t} \tag{52}$$

where

- $Y_{t+k|t}$ is a random variable (in total there will be $t \cdot n_k$ of them at time t when first time was $t = 1$)

- $u_{t+k|t}$ is the input variable
- $\varepsilon_t \sim N(0, \sigma^2)$ and i.i.d. is a random variable (again there will be $t \cdot n_k$ of them at time t when first time was $t = 1$)
- $\beta_{0,k}$ and $\beta_{1,k}$ are the parameters for horizon k

The model is fitted separately for each horizon k using only past data.

Regarding the normal assumption of the error, is not very important, since first of all the least squares method ensures the best estimation of the conditional mean, which is often the wanted and optimal point prediction, see [56]. Regarding the i.i.d. assumption of the errors, this should be checked with the Auto-Correlation Function (ACF) for the one-step ahead residuals, as well as the Cross-Correlation Function (CCF) between the one-step ahead residuals and the inputs, as done by [51]. One of the basic problems is the selction of the optimal model from competing linear regression models. One of the frequently used criteria for model selection is cross-validation.

The k step predictions are

$$\hat{y}_{t+k|t} = \hat{\beta}_{0,k} + \hat{\beta}_{1,k} x_{t+k|t} \tag{53}$$

Note, that the hat is reserved for predictions and estimates calculated using the statistical model, thus the hat is not on the inputs, which are however often predictions (NWPs). If models are fitted in several stages, e.g. the inputs in the final model are actually first predicted using another model, then the hat is removed on the inputs in the final model.

In the above model there are in total $t \cdot n_k$ output (Y) random variables, as well as there are $t \cdot n_k$ error random variables.

Following regression methods are available:

- Least squares
- Recursive least squares (RLS)

however it is planned to also implement:

- Kernel regression (local fitting)
- Quantile regression (estimate quantiles)

The latter opens up the possibilities to calculate probabilistic forecasts (ref), as well as carry out normalization and Copula transformations, which can be very useful for spatio-temporal forecast models (see [58] and [59]).

One note is that when using a recursive update scheme, e.g. RLS, then the parameters are changing over time, which will be indicated with a t on the parameters

$$Y_{t+k|t} = \beta_{0,k,t} + \beta_{1,k,t} x_{t+k|t} + \varepsilon_{t+k|t} \tag{54}$$

6.3.3 Forecast model notation

In this section a suggestion on how to write full description of a forecast model is presented, together with simplified notation. Note that some variables are noted in bold font indicating that they are vectors.

Full notation of the transformation stage

$$\text{Intercept:} \quad \mu_{t+k|t} = 1 \tag{55}$$

$$\text{Periodic:} \quad \boldsymbol{x}^{\text{per}}_{t+k|t} = f_{\text{fs}}(t; n_{\text{har}}) \tag{56}$$

$$\text{Part 1:} \quad x^{\text{nm1}}_{t+k|t} = H(B; a) u^{\text{nm1}}_{t+k|t} \tag{57}$$

$$\text{Part 2:} \quad \boldsymbol{x}^{\text{nm23}}_{t+k|t} = f_{\text{bspline}}(u^{\text{nm2}}_{t+k}; n_{\text{deg}}) u^{\text{nm3}}_{t+k|t} \tag{58}$$

$$\text{Part 3:} \quad \boldsymbol{x}^{\text{nm4}}_{t+k|t} = u^{\text{nm4}}_{t} \tag{59}$$

and the regression stage

$$Y_{t+k|t} = \beta_{0,k}\mu_{t+k|t} + \boldsymbol{\beta}_{1,k}\boldsymbol{x}^{\text{per}}_{t+k|t} + \beta_{2,k}x^{\text{nm1}}_{t+k|t} + \boldsymbol{\beta}_{3,k}\boldsymbol{x}^{\text{nm23}}_{t+k|t} + \varepsilon_{t+k|t} \tag{60}$$

The model inputs are:

- t is simply the time value
- $u^{\text{nm1}}_{t+k|t}$ some forecast input (e.g. NWP variable)
- u^{nm2}_{t+k} some calculated value (e.g. time of day)
- $u^{\text{nm3}}_{t+k|t}$ some forecast input (e.g. NWP variable)
- u^{nm4}_{t} some value known at time t (e.g. an observed variable)

The transformation parameters are

$$\boldsymbol{\theta} = (n_{\text{har}}, a, n_{\text{deg}}) \tag{61}$$

which must be set or optimized (heuristically). In practice, in order to find a good set of parameters, different initialization can be tried along with different algorithms. The dimensionality will be low (i.e. the number of transformation parameters will be few) for most types of generation forecasting, not more than 1 or 2 per input, in [51] the biggest model applied had 5. From previous experience the Nelder-Mean simplex algorithm [60] works well and is very robust, other approaches such as genetic algorithms could useful, since they can also deal with integers. It is left out of scope to deal more in detail with these aspects, since there are plenty of free implementations which can be used.

The regression coefficients are

$$\boldsymbol{\beta}_k = \left[\beta_{0,k} \;\; \beta_{1,1,k} \;\; \beta_{1,2,k} \;\; \cdots \;\; \beta_{1,2n_{\text{har}},k} \;\; \beta_{2,k} \;\; \beta_{3,1,k} \;\; \beta_{3,2,k} \;\; \cdots \;\; \beta_{3,n_{\text{deg}},k} \;\; \beta_{4,k}\right] \tag{62}$$

The full notation where a model is specified in all details can be cumbersome and thus it can be simplified by writing it in a single equation. In all simplifications suggested below, it should then be clearly stated, what is implicit or referenced to a full notation of the model.

The first suggested simplified form is

$$Y_{t+k|t} = \mu_k + f_k^{\text{fs}}(t; n_{\text{har}}) + H_k(B; a)u_{t+k|t}^{\text{nm1}} + f_k^{\text{bspline}}(u_{t+k}^{\text{nm2}}; n_{\text{deg}})u_{t+k|t}^{\text{nm3}} + \beta_k u_t^{\text{nm4}} + \varepsilon_{t+k|t} \tag{63}$$

thus the transformation and regression stage is written implicitly.

To simplify this even more it is suggested to write

$$Y = \mu + f_{\text{fs}}(t; n_{\text{har}}) + H(B; a)u_{\text{nm1}} + f_{\text{bspline}}(u_{\text{nm2}}; n_{\text{deg}})u_{\text{nm3}} + \beta u_{\text{nm4}} + \varepsilon \tag{64}$$

hence removing also the parameters in the transformation functions are removed.

Finally, the most simplified notation suggested is

$$Y = \mu + f_{\text{fs}}(t) + H(B)u_{\text{nm1}} + f_{\text{bspline}}(u_{\text{nm2}})u_{\text{nm3}} + \beta u_{\text{nm4}} + \varepsilon \tag{65}$$

hence removing also the time and horizon indexing.

See the following section for use of the notation in a specific context.

6.4 Examples

Examples of applying the statistical forecasting models are presented: First for observed global radiation and then for solar power for different PV-panel orientations.

6.4.1 Data

Data for the forecasting examples is taken from a data set collected in Sønderborg, Denmark. It comprises Local climate observations and weather forecasts (NWPs). The climate observations are measured at the local district heating plant. The NWPs are from the HIRLAM-S05 model [61] and provided by the Danish Meteorological Institute. All times are in UTC and the time stamp for average values are set to the end of the time interval.

The local climate observations are from a weather station at the district heating plant in Sønderborg, which is less than 10 kilometers from the houses. The data is resampled to hourly average values and the following time series is used:

$$\text{Global radiation: } \left\{G_t^{\text{obs}}; t = 1, \ldots, N\right\} \tag{66}$$

where $N = 21144$ and the unit is $\mathrm{W/m^2}$. For a detailed analysis of the global radiation data used, see [62].

The local climate observations are not used as input in the present examples, only the global radiation is used as model output in the solar forecasting example presented later. They could be setup and combined with the NWPs as described around Equation (36).

6.4.2 Transformation into solar power

Since measurements of solar power was not available for the location and period, then a transformation of the observed global radiation into a the power output of a PV system is carried out. The steps in the transformation are:

- Split the global radiation into a direct radiation and a diffuse signal using the method presented by [63]
- Project the direct radiation from horizontal to a surface with a given slope and azimuth
- Add the projected direct and the horizontal diffuse radiation

Since this approach gives a somewhat too modified signal this is mixed with the global radiation in the proportion 60% and 40% respectively. Finally, this multiplied with some constant to reach the power level of a usual single family building PV-system.

The resulting solar power for PV panels pointing in different orientations are plotted with the observed global radiation in Figure 18, both are normalized. The slope of the panels are in all cases 45 degrees, as if they were mounted on a steep roof. It is clearly seen how the panel pointing towards East has a relatively higher output level in the morning and lower in the afternoon, compared to the global radiation. And for the panel pointing towards West, it is opposite. While the panel pointing South is higher in both the morning and the after noon, due to the tipping of the plane compared to the horizontal plane on which the global radiation is measured.

6.4.3 Numerical weather predictions

The numerical weather predictions (NWPs) used for the forecasting are provided by the Danish Meteorological Institute. The NWP model used is DMI-HIRLAM-S05, which has a 5 kilometer grid and 40 vertical layers [61]. The NWPs consist of time series of hourly values for climate variables, which are updated four times per day and have a 4 hour calculation delay (e.g. the forecast starting at 00:00 is available at 04:00). Since a new two day forecast is calculated every hour, then - in order to use the latest available information - every hour the latest available NWP value for the k'th horizon at time t is picked as

$$\text{Global radiation } (\mathrm{W/m^2}):\ G^{\mathrm{nwp}}_{t+k|t} \tag{67}$$

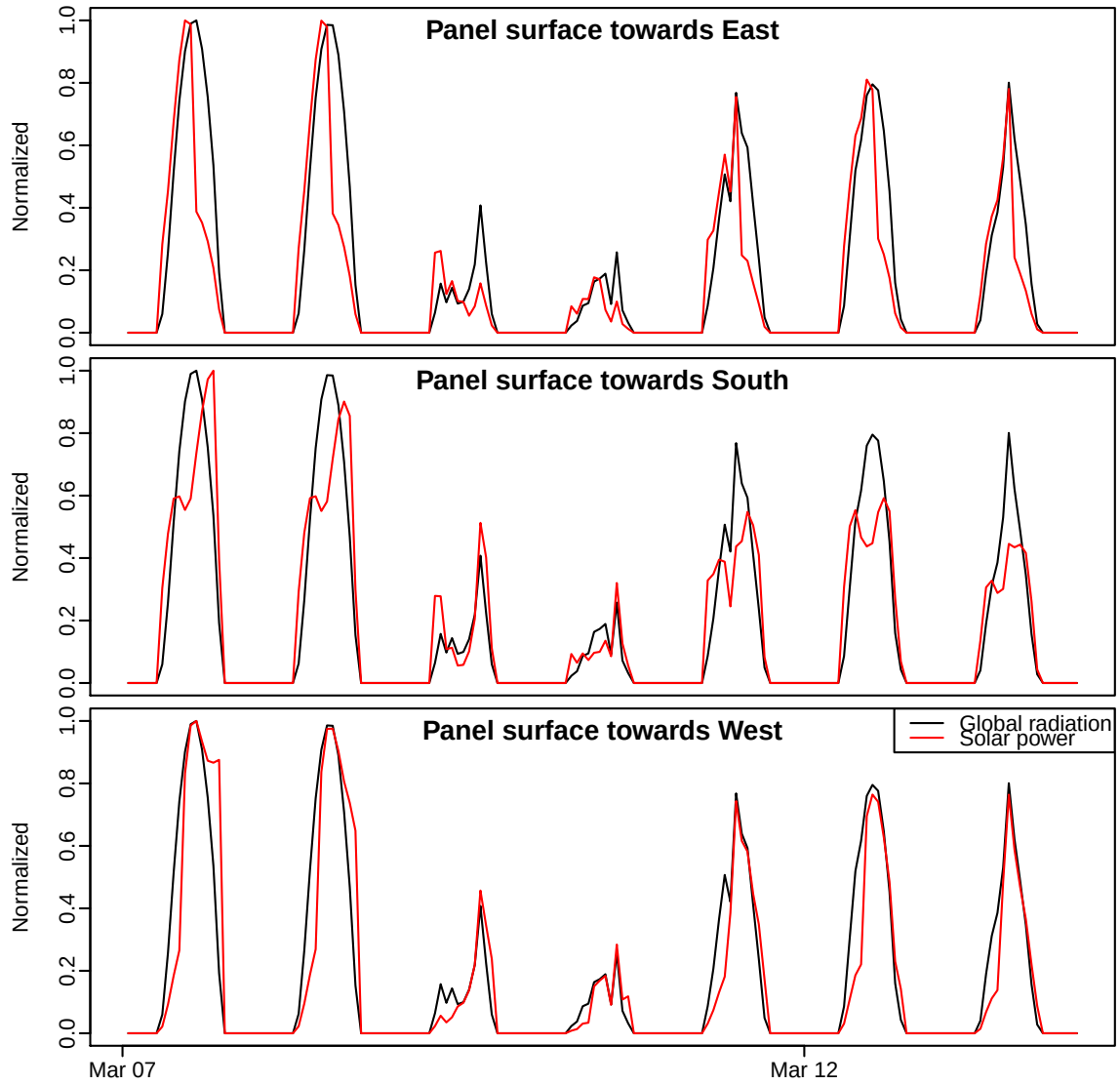

Figure 18: The observed global radiation and solar power, both normalized. The upper plot for a PV panel pointing towards East, the middle plot for a PV panel pointing towards south and finally a PV panel pointing towards West. The period is the first week of April 2011.

This is setup as described in Section 6.2, similarly as for the global radiation in Equation (36), only using purely NWPs (no local observations). Thus the input matrix G_t is formed and used in the examples.

6.4.4 Solar forecasting

The forecast method can be used for solar forecasting, and in this section it is used to forecast first the global radiation and then solar power for the three panel orientations presented above in

Section 6.4.2. Forecast horizons from 1 to 36 hours are calculated. The algorithm uses the basis splines to form a conditional parametric model, in which the functional relationship between the NWPs of global radiation are conditional on the time of day.

The model is the same for all the four setups, but of course it is fitted using the output series, just denoted by Y in the following. Model notation of the transformation stage

$$\text{Global rad. input:} \quad \boldsymbol{x}^{\mathrm{G}}_{t+k|t} = f_{\mathrm{bspline}}(t^{\mathrm{day}}_{t+k}; n_{\mathrm{deg}} = 5) G^{\mathrm{nwp}}_{t+k|t} \tag{68}$$

and the regression stage

$$Y_{t+k|t} = \boldsymbol{\beta}_{1,k} \boldsymbol{x}^{\mathrm{per}}_{t+k|t} + \varepsilon_{t+k|t} \tag{69}$$

The model inputs are:

- t^{day}_{t+k} the time of day, i.e. simply the hour in this case
- $G^{\mathrm{nwp}}_{t+k|t}$ the global radiation NWP

The regression is fitted using the recursive least squares scheme, which thus has the forgetting factor parameter λ. It is optimized in an offline setting as described in [51].

Figure 19 shows different examples of the global radiation forecast. In the upper plot it is seen how the $k = 36$ hours ahead forecasts match the observations for a 2 weeks period. Naturally, it is not perfect, but it is clearly seen how the general pattern is very well modeled. The largest errors occur when the NWP have large errors, hence much of the accuracy of the forecasts depends on the quality of the NWPs.

In the middle plot it is seen how the forecasts, which are updated every hour using the latest available NWPs, do change for particular time points. Thus, as new NWPs become available the forecasts will use this new information. In general the NWPs of shorter horizon are better, however it must be noted that some NWPs used for $k = 1$ hour forecasts are actually 10 hours old, due to NWP calculation time (4 hours in this case) and the fact that the NWPs are only updated every 6 hours. If the latest available observation is also used as an input (an auto-regressive model part), then on shorter horizons the forecasts will become more accurate, as demonstrated in for example [51].

In the lower plot of Figure 19 the $k = 8$ hours forecast is shown for the five day period. It can be seen how there is pattern during the late morning hours, which tend to be lower than in the afternoon, and how the model actually adapts to this pattern.

In Figure 20 the $k = 1$ hour and $k = 36$ hours forecasts are plotted for the solar power for PV panels pointing in different orientations. It is clearly seen how the model adapts to the different patterns of the signals, hence taking automatically into account, the different orientations of the panels. Comparing the $k = 36$ hours forecasts to the same forecasts of global radiation (upper plot of Figure 19), it is seen that the larger errors occur exactly at the same time points, simply because the same NWPs are used and since the errors are propagating through the model.

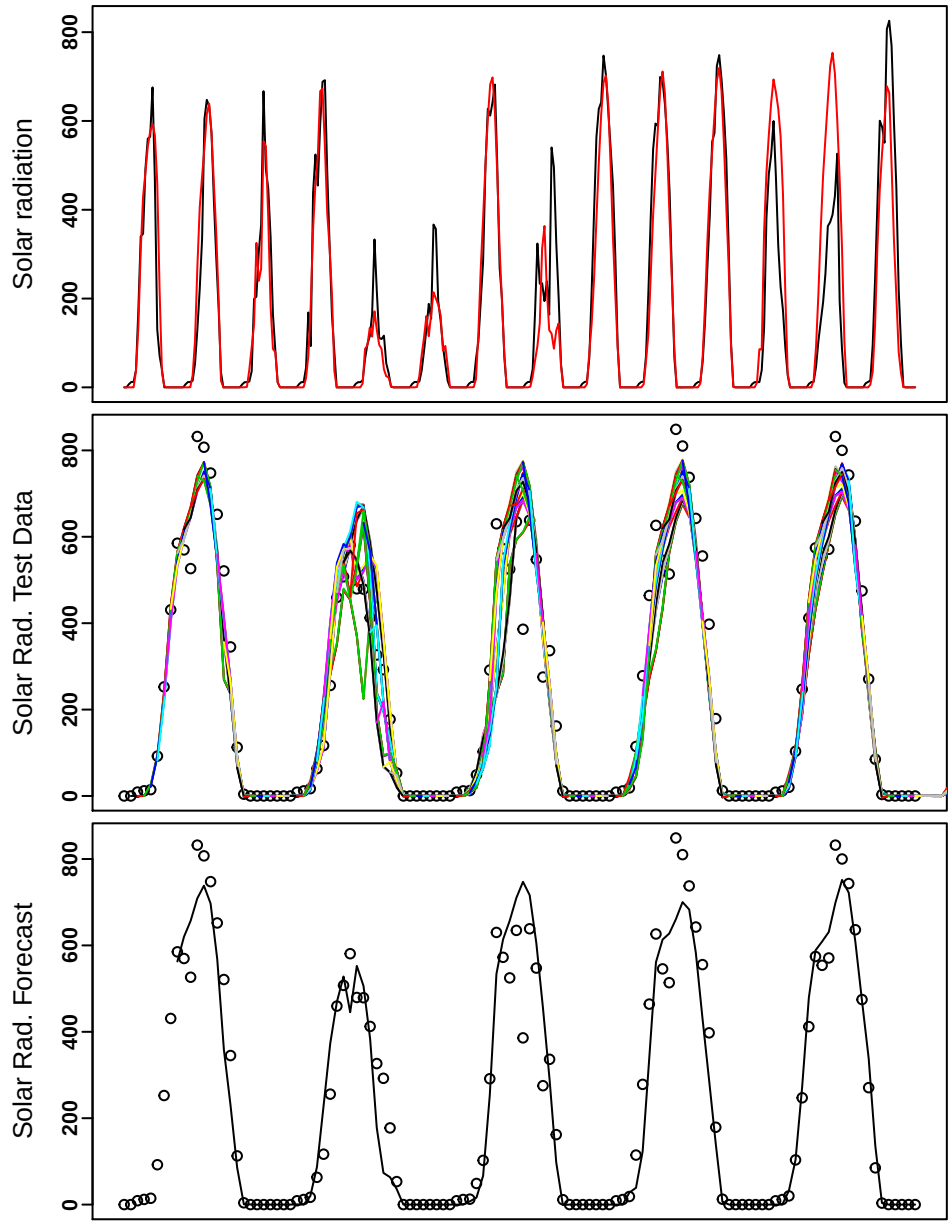

Figure 19: Upper plot: The observed solar radiations in black and the $k = 36$ hours solar radiation forecast in red for the two first weeks of April 2011. Middle plot: All forecasts calculated during 16. to 20. April. Lower plot: The $k = 8$ hours ahead forecast for the same period as in the middle plot.

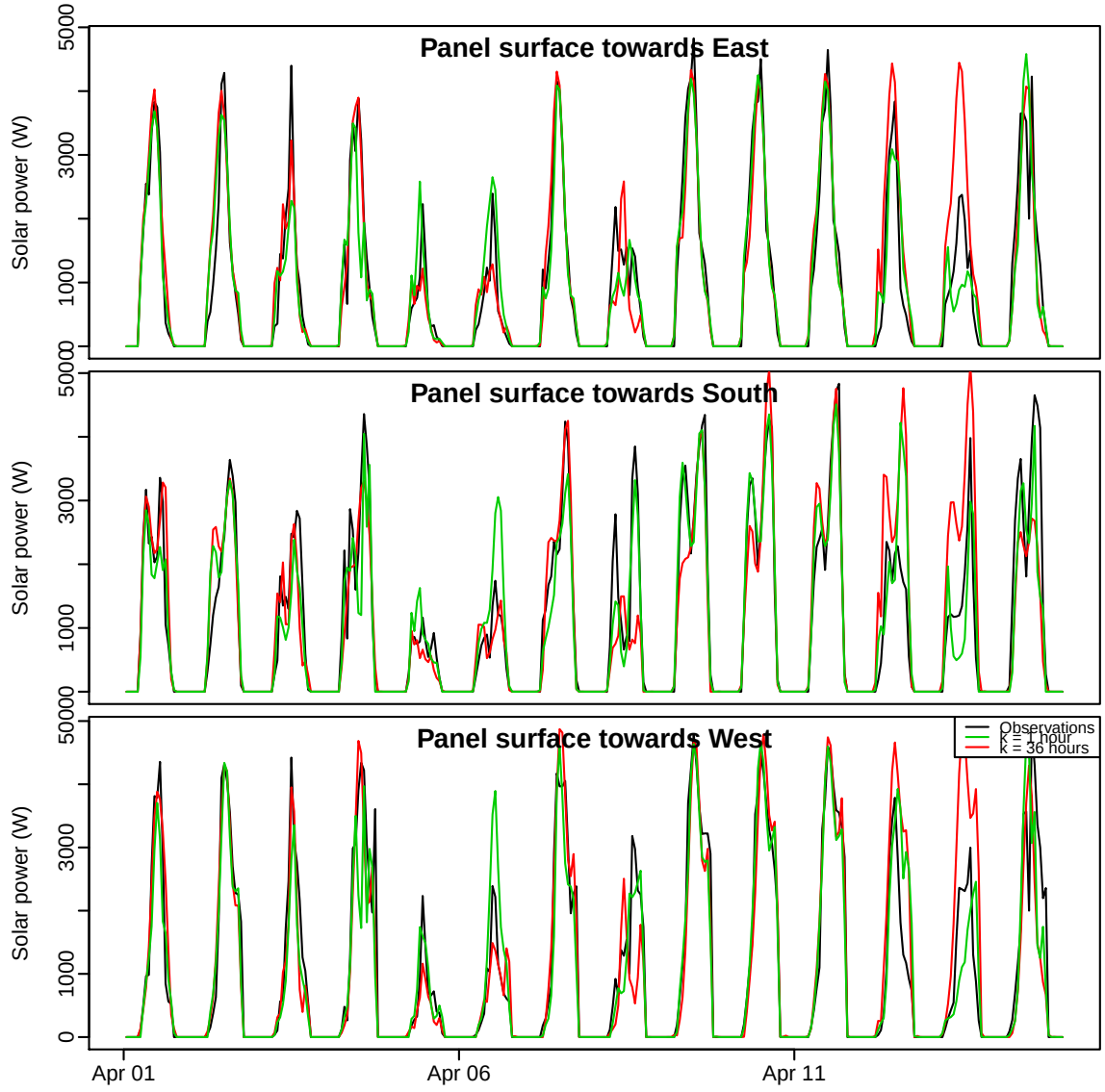

Figure 20: Solar power forecasts for panels pointing in three different orientations. The period is the first two weeks of April 2011.

Table 4: Solar power forecast parameters

PARAMETER	DESCRIPTION	UNITS	TYPE
Input Parameters			
G^{nwp}	Numerical weather predictions of global radiation	W/m^2	Float
P^{sol}	Solar power observations	W	Float
Output Parameters			
$P^{for,sol}$	Solar power forecasts	W	Float

7. CONCLUSION

In this report the models of DERs, which are needed for operating the FLEXCoop pilot sites have been presented. The models cover lighting and HVAC loads, batteries and EVs, as well as PV generation. A detailed description of how to effectively use NWPs as model inputs have been given and of how to setup data-driven models, which can automatically and in a scalable way, adapt to the particular systems. Examples have been given of using the models and algorithms to represent the DERs and forecast the needed variables using the real world data, of course not yet from the pilot sites as they are not established yet, but from other similar systems. It is thereby shown that both load, storage and solar radiation can be modelled accurately and reliable forecast can be generated. Exactly how the models will be setup and tuned for the particular pilot sites depends on which DERs are present there, hence this will be a task which will on going during the remaining of the project.

APPENDIX A: LITERATURE

[1] A. Arif, Z. Wang, J. Wang, B. Mather, H. Bashualdo, and D. Zhao, "Load Modeling – A Review," *IEEE Transactions on Smart Grid*, pp. 1–1, 2017.

[2] L. G. Swan and V. I. Ugursal, "Modeling of end-use energy consumption in the residential sector: A review of modeling techniques," *Renewable and Sustainable Energy Reviews*, vol. 13, no. 8, pp. 1819–1835, Oct. 2009.

[3] "Grant Agreement- 773909, Annex I, Part A, p. 3." 2017.

[4] "Regression analysis," *Wikipedia*. 14-Jun-2018.

[5] NEMA Ballast and Lighting Controls sections, "Energy Savings with Fluorescent and LED Dimming - A NEMA Lighting Systems Division Document LSD 73-2015." .

[6] D. Caicedo, A. Pandharipande, and F. M. J. Willems, "Daylight-adaptive lighting control using light sensor calibration prior-information," *Energy and Buildings*, vol. 73, pp. 105–114, Apr. 2014.

[7] "Home," *Stratego*. [Online]. Available: http://stratego-project.eu/. [Accessed: 04-Jul-2018].

[8] U. Persson, S. Werner, "Quantifying the Heating and Cooling Demand in Europe," Deliverable D2.2 Stratego, WP2, Background Report 4.

[9] S. A. Brown, B. A. Thornton, and S. H. Widder, "Review of Residential Low-Load HVAC Systems," Letter Report PNNL--23017, 1114901, Sep. 2013.

[10] G. Dall'O', *Green Energy Audit of Buildings: A guide for a sustainable energy audit of buildings*. London: Springer-Verlag, 2013.

[11] H. Jin S. J. D. Spitler, "A Parameter Estimation Based Model of Water-to-Water Heat Pumps for Use in Energy Calculation Programs," *ASHRAE Transactions*, p. 16.

[12] V. Badescu, "Model of a space heating system integrating a heat pump, photothermal collectors and solar cells," *Renewable Energy*, vol. 27, no. 4, pp. 489–505, Dec. 2002.

[13] N. T. Gayeski, "Predictive Pre-Cooling Control for Low Lift Radiant Cooling using Building Thermal Mass," PhD Thesis, Massachusetts Institute of Technology, 2010.

[14] C. Verhelst, "Model Predictive Control of Ground Coupled Heat Pump Systems for Office Buildings," PhD Thesis, Katholieke Universiteit Leuven - Faculty of Engineering, 2012.

[15] A. Tsitsanis *et al.*, "Optimal human-centric control strategies," Deliverable WP5, D5.3, Heat4Cool Project.

[16] D Carbonell, J Cadafalch, P Pärisch, and R Consul, "Numerical analysis of heat pumps models. Comperative study between equation-fit and refrigerant cycle based models," in *Conference: Proceedings of the EuroSun*, Rijeka, Croatia, 2012.

[17] Christopher Andrey, Pierre Attard, Régis Bardet, Laurent Fournié, and Paul Khallouf, "Mainstreaming RES - Flexibility Portfolios / Design of flexibility portfolios at Member State level to facilitate a cost-efficient integration of high shares of renewables," European Commission, Directorate-General for Energy, Contract no. ENER/C1/2014-668, Jul. 2017.

[18] K. Cho, "Optimal ESS Scheduling considering Demand Response for Electricity Charge Minimization Under Time of Use Price," *Renewable Energy and Power Quality Journal*, pp. 264–267, May 2016.

[19] A. Eller and A. Dehamna, "'Executive Summary : Market Data : Ancillary Service Markets for Energy Storage Spinning Reserves , Non-Spinning Reserve Capacity , Frequency Regulation , and Volt / VAR Support : Global Market Analysis and Forecasts.'" 2017.

[20] O. M. Longe, K. Ouahada, S. Rimer, A. N. Harutyunyan, and H. C. Ferreira, "Distributed demand side management with battery storage for smart home energy scheduling," *Sustainability (Switzerland)*, vol. 9, no. 1, 2017.
[21] W. Steel, "Energy Storage Market Outlook 2017: State of Play," *renewableenergyworld.com*, 2017. [Online]. Available: https://www.renewableenergyworld.com/articles/print/volume-20/issue-1/features/storage/energy-storage-market-outlook-2017-state-of-play.html.
[22] Kokam, "Battery for Home Energy Storage System." [Online]. Available: http://kokam.com/khess/.
[23] Enphase, "The Enphase Storage System." [Online]. Available: https://enphase.com/en-us/products-and-services/storage.
[24] VARTA, "VARTA Energy Storage Systems." [Online]. Available: https://www.varta-storage.com/products/energy/?lang=en.
[25] TESLA, "POWERWALL." [Online]. Available: https://www.tesla.com/es_ES/powerwall?redirect=no.
[26] EnerSys, "Home Energy Storage Solutions." [Online]. Available: http://www.enersys-emea.com/reserve/pdf/EN-HESS-BR-001_0615.pdf.
[27] S. Kumar and R. Y. Udaykumar, "Stochastic Model of Electric Vehicle Parking Lot Occupancy in Vehicle-to-grid (V2G)," *Energy Procedia*, vol. 90, no. December 2015, pp. 655–659, 2015.
[28] D. Steward, "Critical Elements of Vehicle-to- Grid (V2G) Economics Critical Elements of Vehicle-to- Grid (V2G) Economics," no. September, 2017.
[29] W. Kempton and S. E. Letendre, "Electric vehicles as a new power source for electric utilities," *Transportation Research Part D: Transport and Environment*, vol. 2, no. 3, pp. 157–175, 1997.
[30] Z. Wang and S. Wang, "Grid power peak shaving and valley filling using vehicle-to-grid systems," *IEEE Transactions on Power Delivery*, vol. 28, no. 3, pp. 1822–1829, 2013.
[31] B. K. Sovacool and R. F. Hirsh, "Beyond batteries: An examination of the benefits and barriers to plug-in hybrid electric vehicles (PHEVs) and a vehicle-to-grid (V2G) transition," *Energy Policy*, vol. 37, no. 3, pp. 1095–1103, 2009.

[32] G. Box, G. Jenkins, and G. Reinsel, *Time series analysis*. Holden-day San Francisco, 1976.

[33] H. Madsen, *Time Series Analysis*. Chapman & Hall/CRC, 2007.

[34] G. P. Zhang, "Time series forecasting using a hybrid arima and neural network model," *Neurocomputing*, vol. 50, pp. 159–175, 2003.

[35] H. Tong, *Threshold models in non-linear time series analysis*, vol. 21. Springer Science & Business Media, 2012.

[36] B. Chowdhury and S. Rahman, "Forecasting sub-hourly solar irradiance for prediction of photovoltaic output," in *IEEE Photovoltaic Specialists Conference, 19th, New Orleans, LA, May 4-8, 1987, Proceedings (A88-34226 13-44). New York, Institute of Electrical and Electronics Engineers, Inc., 1987, p. 171-176.*, pp. 171–176, 1987.

[37] A. Sfetsos and A. Coonick, "Univariate and multivariate forecasting of hourly solar radiation with artificial intelligence techniques," *Solar Energy*, vol. 68, no. 2, pp. 169–178, 2000.

[38] D. Heinemann, E. Lorenz, and M. Girodo, "Forecasting of solar radiation," in *Solar Resource Management for Electricity Generation from Local Level to Global Scale* (E. Dunlop, L. Wald, and M. Suri, eds.), (New York), pp. 83–94, Nova Science Publishers, 2006.

[39] E. Lorenz, D. Heinemann, H. Wickramarathne, H. Beyer, and S. Bofinger, "Forecast of ensemble power production by grid-connected pv systems," in *Proc. 20th European PV Conference, September 3-7, 2007, Milano*, 2007.

[40] F. O. Hocaoglu, O. N. Gerek, and M. Kurban, "Hourly solar radiation forecasting using optimal coefficient 2-d linear filters and feed-forward neural networks," *Solar Energy*, vol. 82, no. 8, pp. 714–726, 2008.

[41] J. Cao and X. Lin, "Study of hourly and daily solar irradiation forecast using diagonal recurrent wavelet neural networks," *Energy Conversion and Management*, vol. 49, no. 6, pp. 1396–1406, 2008.

[42] N. Sharma, P. Sharma, D. Irwin, and P. Shenoy, "Predicting solar generation from weather forecasts using machine learning," in *Smart Grid Communications (SmartGridComm), 2011 IEEE International Conference on*, pp. 528–533, Oct 2011.

[43] A. Ragnacci, M. Pastorelli, P. Valigi, and E. Ricci, "Exploiting dimensionality reduction techniques for photovoltaic power forecasting," in *Energy Conference and Exhibition (ENERGYCON), 2012 IEEE International*, pp. 867–872, Sept 2012.

[44] R. Marquez and C. F. Coimbra, "Forecasting of global and direct solar irradiance using stochastic learning methods, ground experiments and the nws database," *Solar Energy*, vol. 85, no. 5, pp. pp. 746–756, 2011.

[45] H. T. Pedro and C. F. Coimbra, "Assessment of forecasting techniques for solar power production with no exogenous inputs," *Solar Energy*, vol. 86, no. 7, pp. pp. 2017–2028, 2012.

[46] M. Zamo, O. Mestre, P. Arbogast, and O. Pannekoucke, "A benchmark of statistical regression methods for short-term forecasting of photovoltaic electricity production. part II: Probabilistic forecast of daily production," *Solar Energy*, vol. 105, pp. pp. 804–816, 2014.

[47] M. P. Almeida, O. Perpion, and L. Narvarte, "PV power forecast using a nonparametric PV model," *Solar Energy*, vol. 115, pp. pp. 354–368, 2015.

[48] H. Nielsen, H. Madsen, and D. E. F. P. og Fordeling af El og Varme, "Predicting the heat consumption in district heating systems using meteorological forecasts," tech. rep., DTU IMM, 2000.

[49] H. A. Nielsen and H. Madsen, "Modelling the heat consumption in district heating systems using a grey-box approach," *Energy & Buildings*, vol. 38, no. 1, pp. 63–71, 2006.

[50] P. Bacher, H. Madsen, and H. A. Nielsen, "Online short-term solar power forecasting," *Solar Energy*, vol. 83, no. 10, pp. 1772–1783, 2009.

[51] P. Bacher, H. Madsen, H. A. Nielsen, and B. Perers, "Short-term heat load forecasting for single family houses," *Energy and Buildings*, vol. 65, no. 0, pp. 101–112, 2013.

[52] P. Bacher, H. Madsen, and H. Aalborg Nielsen, "Load forecasting for supermarket refrigeration," tech. rep., DTU Compute, 2013.

[53] P. Vogler-Finck, P. Bacher, and H. Madsen, "Online short-term forecast of greenhouse heat load using a weather forecast service," *Applied Energy*, vol. 205, pp. 1298 – 1310, 2017.

[54] T. Nielsen, H. Madsen, H. A. Nielsen, P. Pinson, G. Kariniotakis, N. Siebert, I. Marti, M. Lange, U. Focken, L. V. Bremen, *et al.*, "Short-term wind power forecasting using advanced statistical methods," in *Proceedings of The European Wind Energy Conference, EWEC 2006*, 2006.

[55] H. Nielsen, T. Nielsen, and H. Madsen, "An overview of wind power forecasts types and their use in large-scale integration of wind power," in *Proceedings of the 10th International Workshop on Large-Scale Integration of Wind Power into Power Systems*, 2011.

[56] H. Madsen, *Time series analysis*. Chapman and Hall/CRC, 2008.

[57] T. Hastie, R. Tibshirani, J. Friedman, T. Hastie, J. Friedman, and R. Tibshirani, *The elements of statistical learning*, vol. 2. Springer, 2009.

[58] P. Pinson, H. Madsen, H. A. Nielsen, G. Papaefthymiou, and B. Klöckl, "From probabilistic forecasts to statistical scenarios of short-term wind power production," *Wind energy*, vol. 12, no. 1, pp. 51–62, 2009.

[59] E. B. Iversen, J. M. Morales, J. K. Møller, P.-J. Trombe, and H. Madsen, "Leveraging stochastic differential equations for probabilistic forecasting of wind power using a dynamic power curve," *Wind Energy*, vol. 20, no. 1, pp. 33–44, 2017.